Supporting Information

Rational Design of a Red-Light Absorbing Ruthenium Polypyridine Complex as a Photosensitizer for Photodynamic Therapy

Alessia Fennes,[a] *Nicolás Montesdeoca,*[a] *Zisis Papadopoulos,*[a] *Johannes Karges*[a,]*

[a] Faculty of Chemistry and Biochemistry, Ruhr-University Bochum, Universitätsstrasse 150, 44780 Bochum, Germany.

* Email: johannes.karges@ruhr-uni-bochum.de, Tel: +49 2343224187; WWW: www.kargesgroup.ruhr-uni-bochum.de

EXPERIMENTAL SECTION

Computational details

The geometry of the metal complexes was determined using density-functional theory calculations and excited states were determined using time-dependent density-functional theory calculations with the Gaussian 16 software package. (Gaussian 16, Revision C.01, M. J. Frisch, G. W. Trucks, H. B. Schlegel, G. E. Scuseria, M. A. Robb, J. R. Cheeseman, G. Scalmani, V. Barone, G. A. Petersson, H. Nakatsuji, X. Li, M. Caricato, A. V. Marenich, J. Bloino, B. G. Janesko, R. Gomperts, B. Mennucci, H. P. Hratchian, J. V. Ortiz, A. F. Izmaylov, J. L. Sonnenberg, D. Williams-Young, F. Ding, F. Lipparini, F. Egidi, J. Goings, B. Peng, A. Petrone, T. Henderson, D. Ranasinghe, V. G. Zakrzewski, J. Gao, N. Rega, G. Zheng, W. Liang, M. Hada, M. Ehara, K. Toyota, R. Fukuda, J. Hasegawa, M. Ishida, T. Nakajima, Y. Honda, O. Kitao, H. Nakai, T. Vreven, K. Throssell, J. A. Montgomery, Jr., J. E. Peralta, F. Ogliaro, M. J. Bearpark, J. J. Heyd, E. N. Brothers, K. N. Kudin, V. N. Staroverov, T. A. Keith, R. Kobayashi, J. Normand, K. Raghavachari, A. P. Rendell, J. C. Burant, S. S. Iyengar, J. Tomasi, M. Cossi, J. M. Millam, M. Klene, C. Adamo, R. Cammi, J. W. Ochterski, R. L. Martin, K. Morokuma, O. Farkas, J. B. Foresman, and D. J. Fox, Gaussian, Inc., Wallingford CT, 2016). The calculations were performed using the global hybrid B3LYP potential in conjunction with the Los Alamos LANL2 effective core potential and the corresponding triple-zeta basis set for the Ruthenium atom. Solvent effects were included using a polarizable continuum model (PCM). The structures of all calculated molecules correspond to ground state minima on the ground state potential energy surfaces with no imaginary frequencies present. Absorption spectra were modelled by convolution with Gaussian functions having a full width at half maximum (FWHM) of 0.3 eV.

Materials and Methods

All chemicals were obtained from commercial sources and used without further purification. All syntheses were performed under an argon atmosphere in dried Schlenk flasks using dry solvents. Light-sensitive reactions were conducted in the absence of light by wrapping the apparatus in aluminum foil. Thin-layer chromatography was carried out using Merck TLC aluminum sheets. Column chromatography was performed with silica gel 60 M (0.04-0.063 mm, Macherey-Nagel) at atmospheric pressure. The solvents and Rf values used for chromatography are detailed in the corresponding experimental section. Thin-layer

chromatography analysis, including substance detection, was performed using fluorescence detection under UV light (wavelength λ = 254 nm). ^{1}H NMR and ^{13}C NMR spectra were recorded using a Bruker Avance Neo 300 MHz at 298.15 K. Chemical shifts are reported in parts per million (ppm) relative to the ^{1}H signals of the deuterated solvents.

Synthesis of $[Ru(DMSO)_4(Cl)_2]$

The compound was prepared using a similar procedure as previously reported (I. P. Evans, A. Spencer, G. Wilkinson *J. Chem. Soc. Dalton Trans.* **1973**, 204-209). Ruthenium(III)-chloride hydrate (2 g, 7.64 mmol, assuming $xH_2O = 3$) was partially dissolved in ethanol (50 mL) and refluxed for 3 hours protected from light. The compound dissolved completely, and the color changed from brown to deep green. The solvent was evaporated, and an oily green residue was obtained which was mix with dimethyl sulfoxide (8 mL). The mixture was heated at 150 °C for 2 hours protected from light. A color change from dark green to yellow was observed. Then, the solution was cooled down to room temperature and acetone (100 ml) was added. The mixture was placed in the fridge overnight and the crude product precipitated as a bright yellow powder. The product was collected by filtration and washed with acetone (20 mL). To obtain more product, the filtrate was evaporated, acetone (50 mL) was added, and the mixture was placed in the fridge overnight. More product was obtained, collected, and washed as before. This procedure was repeated three times to yield the maximum amount of product. 3.48 g (7.1 mmol, 72%) of $[Ru(DMSO)_4(Cl)_2]$ were yielded as a bright yellow powder. ^{1}H-NMR (400 MHz, D_2O): δ = 3.52 (s, 6H), 3.50 (s, 6H), 3.42 (s, 6H), 2.75 (s, 6H) ppm; ^{13}C-NMR (101 MHz, D_2O): δ = 46.8, 46.6, 45.7, 45.2, 44.7, 44.4, 38.7 ppm.

Synthesis of $[Ru(2,2'\text{-bipyridine})_2(Cl)_2]$

The compound was prepared using a similar procedure as previously reported (C. E. McCusker, J. K. McKusker *Inorg. Chem.* **2011**, *50*, 1656-1669). $[Ru(DMSO)_4Cl_2]$ (1800 mg, 3.72 mmol, 1.00 eq.), 2,2′-bipyridine (1044 mg, 6.69 mmol, 1.8 eq.), and LiCl (14.18 g) were dissolved in dry *N*,*N*-dimethylformamide (50 mL) protected from light and under nitrogen atmosphere. The mixture was refluxed for 4 hours until the solution turned dark purple. Then the solution was cooled down to room temperature and acetone (500 mL) was added. The mixture was placed in the freezer overnight and the crude product precipitated. The product was collected by filtration

and washed with distilled water (~100 mL) to remove the excess of LiCl and unwanted [Ru(2,2′-bipyridine)$_3$]$^{2+}$. Finally, the product was washed with diethyl ether and dried under vacuum. A solid dark purple powder was obtained (1080 mg, 2.23 mmol, 60%). ^{1}H-NMR (400 MHz, DMSO): δ = 9.97 (d, *J* = 4.1 Hz, 2H), 8.63 (d, *J* = 8.1 Hz, 2H), 8.48 (d, *J* = 7.1 Hz, 2H), 8.06 (t, *J* = 7.8 Hz, 2H), 7.76 (t, *J* = 6.6 Hz, 2H), 7.67 (t, *J* = 7.8 Hz, 2H), 7.51 (d, *J* = 4.5 Hz, 2H), 7.10 (t, *J* = 6.6 Hz, 2H) ppm; ^{13}C-NMR (101 MHz, DMSO): δ = 160.2, 158.2, 153.2, 152.0, 134.6, 133.3, 125.3, 125.3, 122.8, 122.5 ppm.

Synthesis of (*E,E′*)-4,4'-bis[p-(*N,N*-phenylamino)styryl]-2,2'-bipyridine

In a flask with argon atmosphere, 4,4-dimethyl-2,2′-bipyridine (50 mg, 271.4 µmol, 1.0 equiv.) was dissolved in *N,N*-dimethylformamide (1.8 mL). Then, 4-(Diphenylamino)benzaldehyde (138.8 µL, 597.0 µmol, 2.2 equiv.) was added to the solution. Afterward, potassium tert-butoxide (121.8 mg, 1.1 mmol, 4.0 equiv.) was added slowly. The mixture was stirred at room temperature for 24 h. After that, the mixture was poured into water (20 mL) and the suspension cooled down to 5°C for 2 h. The insoluble precipitate was filtered and washed with water and methanol (1 mL). The crude product was co-evaporated with n-heptane to remove traces of *N,N*-dimethylformamide. The residue was dried under a high vacuum. The product was purified by recrystallization from boiling acetic acid. A solid yellow powder was obtained (102.3 mg, 64%). ^{1}H-NMR (300 MHz, DCM-d$_2$): δ = 8.65 (d, J = 5.2 Hz, 2H), 8.59 (s, 2H), 7.52 (s, 2H), 7.49 (s, 1H), 7.47 (d, J = 16.4 Hz, 4H), 7.43 (d, J = 1.7 Hz, 1H), 7.37-7.30 (m, 8H), 7.18-7.06 (m, 18H) ppm; ^{13}C-NMR (75 MHz, DCM-d$_2$): δ = 156.9, 149.9, 147.7, 146.3, 133.0, 129.8, 128.4, 125.3, 124.4, 123.9, 123.1, 121.1, 118.2 ppm; ESI-HRMS (pos. detection mode): calcd. for $C_{50}H_{39}N_4$ [M+H]$^+$ m/z 695.3175; found: 695.3189.

Synthesis of [Ru(2,2′-bipyridine)$_2$((*E,E′*)-4,4'-bis[p-(*N,N*-phenyl-amino)styryl]-2,2'-bipyridine)][PF$_6$]$_2$

(*E,E′*)-4,4'-bis[p-(*N,N*-phenylamino)styryl]-2,2'-bipyridine (100.0 mg, 206.5 mmol, 1.0 equiv.) and Ru(2,2′-bipyridine)$_2$Cl$_2$ (172.2 mg, 247.8 mmol, 1.2 equiv.) were suspended in dry ethanol (50 mL) under nitrogen atmosphere and the mixture was heated at reflux for 24 h. Then the solution was cooled down to room temperature and the insoluble precipitate was removed by filtration. To the residual solution, a saturated aqueous solution of ammonium hexafluorophosphate was added until no precipitation was observed anymore. The crude

product, which precipitated as a hexafluorophosphate salt, was collected by centrifugation and washed with ethanol, water, and diethyl ether. The crude product was purified via column chromatography with gradient acetonitrile and aqueous potassium nitrate solution (0.4 M) 10:1. The fractions containing the product were united and the solvent was removed under reduced pressure. The residue was dissolved in acetonitrile and undissolved potassium nitrate was removed by filtration. The solid was dissolved in water and a saturated aqueous solution of ammonium hexafluorophosphate was added until no precipitation was observed anymore. The crude product, which precipitated as a hexafluorophosphate salt, was collected by centrifugation and washed with water and diethyl ether. A solid red powder was obtained (22.9 mg, 10%). R_f -value (CH_3CN/aq. KNO_3 (0.4 M) 10:1): 0.33. ^{1}H-NMR (400 MHz, Acetonitrile-d_3): δ = 8.73 (s, 2H,), 8.51 (d, J = 8.1 Hz, 4H), 8.05 (t, J = 7.5 Hz, 4H), 7.84 (d, J = 5.5 Hz, 2H), 7.70 (d, J= 17.0 Hz, 4H), 7.57-7.53 (m, 6H), 7.16 (d, J = 2.8 Hz, 2H), 7.12 (m, 12H), 6.99 (d, J = 8.8 Hz, 4H) ppm; ^{13}C-NMR (100 MHz, Acetonitrile-d_3): δ = 158.1, 158.0, 152.7, 152.1, 150.3, 148.2, 148.0, 138.7, 137.1, 130.6, 130.0, 129.7, 128.54, 128.52, 126.3, 125.2, 125.1, 124.9, 122.7, 122.6, 121.4 ppm; ESI-HRMS (pos. detection mode): calcd. for $C_{70}H_{54}N_8Ru$ $[M]^{2+}$ m/z 554.1752; found: 554.1767; Elemental analysis calcd. for $C_{70}H_{54}F_{12}N_8P_2Ru$ (%): C 60.13, H 3.89, N 8.01; found: C 59.73, H 3.74, N 7.76.

Emission Quantum Yield

For the determination of the emission quantum yield, the metal complex was dissolved in degassed water with an absorbance of 0.1 at 420 nm. This solution was irradiated in fluorescence quartz cuvettes (width 1 cm) with a Jasco Spectrofluorometer FP-8300 at 420 nm. The emission quantum yields were determined by comparison with the reference $[Ru(bipy)_3]Cl_2$ in water (Φ_{em}=4.0%) applying the following formula:

$$\Phi_{em,\,sample} = \Phi_{em,\,reference} * (F_{reference} / F_{sample}) * (I_{sample} / I_{reference}) * (n_{sample} / n_{reference})^2$$

$$F = 1 - 10^{-A}$$

Φ_{em} = luminescence quantum yield, F = fraction of light absorbed, I = integrated emission intensities, n = refractive index, A = absorbance of the sample at irradiation wavelength.

Singlet Oxygen Production

The singlet oxygen production was carried out via the decomposition of 1,3-diphenylisobenzofuran (410 nm absorption maximum decrease). For the measurements, a 1% saturated solution of 1,3-diphenylisobenzofuran was prepared in acetonitrile. The UV/Vis spectra were recorded using a Shimadzu UV-1900 spectrophotometer, equipped with Hellma optical fibers and two Thorlabs KSC101 shutters (one in the instrument and one in the Arc lamp beamline). Irradiation was performed using a 150 W Xe-Arc discharge lamp with a 590 nm long-pass filter, resulting in an irradiance of 100 µW/cm². An absorption spectrum was recorded prior to irradiation and repeated at the specified time intervals. The setup was tested for 60 minutes with a 1% saturated 1,3-diphenylisobenzofuran solution in acetonitrile containing 0.1% dimethyl sulfoxide, without the addition of any compound. No degradation of 1,3-diphenylisobenzofuran was observed during this period. During irradiation, spectra were recorded every 5 minutes, showing a consistent degradation of 1,3-diphenylisobenzofuran as indicated by the continuous decrease in the maximum absorbance at 410 nm.

Stability in Water

The stability of the compounds in water was determined by UV/Vis absorption spectroscopy. The compound was dissolved in water and stored at room temperature in the dark. The absorption spectrum from 250-650 nm was recorded with a Shimadzu UV-1900i Spectrometer after each time interval (0, 24, 48 h) and compared.

Stability upon Irradiation

The photostability of [Ru(2,2′-bipyridine)$_2$((*E,E′*)-4,4'-bis[p-(*N,N*-phenyl-amino)styryl]-2,2'-bipyridine)][PF_6]$_2$ (15 µM) in water was determined by UV/Vis absorption spectroscopy. The UV/Vis spectra were recorded using a Shimadzu UV-1900 spectrophotometer, equipped with Hellma optical fibers and two Thorlabs KSC101 shutters (one in the instrument and one in the Arc lamp beamline). Irradiation was performed using a 150 W Xe-Arc discharge lamp with a 420 nm long-pass filter, resulting in an irradiance of 100 µW/cm². The absorption spectrum from 250-650 nm was recorded after various irradiation time intervals (0-60 min). The absorption spectra of [Ru(2,2'-bipyridine)$_3$]Cl_2 (7.5 µM) and Photofrin (10 µM) were measured for comparative purposes.

Complementary, the photostability of [Ru(2,2′-bipyridine)$_2$((*E,E′*)-4,4'-bis[p-(*N,N*-phenyl-amino)styryl]-2,2'-bipyridine)][PF_6]$_2$ was determined by ^{1}H-NMR spectroscopy. ^{1}H-NMR was

recorded in a Brucker Ascend™ 400 WB in D_2O. ^{1}H-NMR spectra were recorded before and after irradiation for 60 min. Irradiation was performed using a 150 W Xe-Arc discharge lamp with a 420 nm long-pass filter, resulting in an irradiance of 100 μW/cm².

Distribution Coefficient

The lipophilicity of the metal complexes was determined by measuring its distribution coefficient between the phosphate-buffered saline and octanol phase by using the "shake-flask" method. For this technique, the used phases were previously saturated in each other. The complex was dissolved in the phase (A) with its major presence with an absorbance of about 0.5 at 350 nm. This solution was then mixed with an equal volume of the other phase (B) at 300 rpm for 12 h and then equilibrated overnight. The phase A was then carefully separated from phase B. The amount of the complex before and after the sample mixing was determined by UV/Vis absorption spectroscopy at 350 nm using a Jasco V-670 spectrophotometer. The evaluation of the complexes was repeated three times and the ratio between the organic and aqueous phases was calculated. It is important to note that the selected intensity and wavelengths are in the Lambert-Beer range.

$$logP = log\frac{C_O}{C_W} = log\frac{I_O}{I_W}$$

c = concentration, I = intensity. The calculation was based on the intensity where I_0 is the intensity of the substance in the octanol-rich phase and I_W is the intensity of the substance in the water-rich phase.

Parallel Artificial Membrane Permeability Assay

The cell permeability of the metal complexes was assessed using an artificial membrane using a slight modification to a reported protocol (M. Kansy, F. Senner, K. Gubernator, *J. Med. Chem.* **1998**, *41*, 1007-1010). The wells in the acceptor plate were filled with phosphate-buffered saline solution (300 μL). 4% Lecithin in dodecane (5 μL) was carefully placed on top of the membrane of the donor plate. The metal complex (200 μL, 100 μM) diluted in water was added into the wells of the donor plate. The tray of the donor plate was placed inside the acceptor plate. The combined plates were incubated for 8 h at room temperature in the dark. The donor plate was removed and the absorbance at 350 nm in each well in the acceptor plate was determined using a Jasco V-670 spectrophotometer. As control substances, commercially supplied reference

compounds with high (0.055±0.005 μm/s), medium (0.028±0.004 μm/s), and low (0.009±0.002 μm/s) cell permeability were used. Using the following equation, the permeability rate of the compound was determined:

$$P = \frac{VD * VA}{(VD + VA) * Area * time} * -\ln\left(1 - \frac{ODA}{ODE}\right)$$

P = permeability rate in cm/s, VD = donor volume (0.2 cm^3), VA = acceptor volume (0.3 cm^3), Area = 0.24 cm^2, time = incubation time in s, ODA = absorbance of acceptor solution, ODE = absorbance of equilibrated acceptor solution.

Cell Culture

All cell lines were obtained from the German Cancer Research Center (Deutsches Krebsforschungszentrum, DKFZ). Murine mouse colon carcinoma cells (CT-26) cells were cultured in RPMI 1640 medium supplemented with 10% FBS Superior and 2% penicillin/streptomycin. Human breast adenocarcinoma cells (MCF-7), and human pancreas adenocarcinoma cells (PT-45) were cultured in DMEM medium (4.5 g/L D-Glucose, L-Glutamine) supplemented with 10% FBS Superior, 2.4% penicillin/streptomycin, 1.2% GlutaMAX-I and 1% sodium pyruvate. Human fibroblasts (GM-5657) cells were cultured in DMEM medium (1 g/L D-Glucose) supplemented with 10% FBS Superior, 2.4% penicillin/streptomycin, 1.2% GlutaMAX-I and 1% sodium pyruvate. LGC Standards Ltd. provided all the cell lines, which were cultured at 37 °C with 10% CO2. Prior to each experiment, the cells were passaged at least 3 times.

(Photo-)toxicity on 2D Cell Monolayers

A total of 6×10^3 cells were seeded onto 96-well plates and allowed to adhere overnight. The cells were treated with the metal complex which was diluted in cell media to a total volume of 200 μL. The cells were treated with increasing concentrations of the metal complex diluted in cell media achieving a total volume of 200 μL for 4 h at 37 °C and 10% CO_2. The cells were incubated with the metal complex for 4 h and after this time the medium refreshed. To study the phototoxic effect of the metal complex, the cells were exposed to blue (450 nm, power: 20%, 10 min, 1.2 J/cm^2) or red (630 nm, power: 10%, 15 min, 0.9 J/cm^2) light irradiation. To

study the dark cytotoxicity effect of the metal complex, the cells were not irradiated and after the incubation time, the medium was exchanged. The cells were grown for an additional 44 h at 37 °C and 10% CO_2. After the specified incubation period, the culture medium was substituted with phosphate-buffered saline buffer containing 3-(4,5-Dimethylthiazol-2-yl)-2,5-diphenyltetrazolium bromide (MTT) with a final concentration of 12 µM. The cells were incubated for 2 h at 37 °C and 10% CO_2 and the mixture was replaced by 200 µL DMSO. The concentration of the formazan dissolved in DMSO was determined with an Infinite M Nano plus Microplate reader (Tecan).

Light-Induced Generation of Reactive Oxygen Species in 2D Cell Monolayers

A total of 2.5 × 105 cells were seeded onto an 8-well plate and allowed to adhere overnight. The cells were treated with the metal complex which was diluted in cell media to a total volume of 200 µL for 2 h. The cells were incubated with the metal complex for 4 h and after this time the medium refreshed. To study the light-induced effect of the metal complex, the cells were exposed to red (630 nm, power: 10%, 7.5 min, 0.45 J/cm^2) light irradiation. To study the dark effect of the metal complex, the cells were not irradiated and after the incubation time, the medium was exchanged. To assess the generation of reactive oxygen species, the cells were incubated with phosphate-buffered saline buffer containing 2',7'-dichlorodihydrofluorescein diacetate with a final concentration of 5 µM at 37 °C and 10% CO_2 for 30 minutes and imaged by fluorescence microscopy. The camera was mounted on an Olympus IX81 inverted fluorescence microscope equipped with various fluorescence filters. All images were recorded with a 10x objective and 1x ocular. λ_{ex} = 460-490 nm, λ_{em} = 517-527 nm.

Generation and Analysis of 3D Multicellular Tumor Spheroids

A suspension of 0.75% agarose in PBS was heated inside a high-pressure autoclave. The hot emulsion was transferred into a 96-well plate (50 µL per well). The plates were exposed for 3h to UV irradiation and allowed to cool down. After this time, a cell suspension of 3 × 10^4 cells was seeded on top of the agarose ground layer. Within two to three days multicellular tumor spheroids were formed from the cell suspension. The multicellular tumor spheroids were cultivated and maintained at 37 °C in a cell culture incubator at 37 °C with 5% CO_2 atmosphere. The culture medium was replaced every two days. The formation, integrity, diameter, and

volume of the multicellular tumor spheroids were monitored. The volume was calculated using the following equation: $V = 4/3\pi r3$.

(Photo-)toxicity on 3D Multicellular Tumor Spheroids

The cytotoxicity of the compounds in multicellular tumor spheroids was assessed by measurement of the adenosine triphosphate concentration. Multicellular tumor spheroids were treated with increasing concentrations of the compound by replacing 50% of the media with drug-supplemented media. To study the phototoxic effect of the metal complex, the multicellular tumor spheroids were exposed to red (630 nm, power: 10%, 15 min, 0.9 J/cm^2) light irradiation. To study the dark cytotoxicity effect of the metal complex, the cells were not irradiated. The multicellular tumor spheroids were incubated for 44 h at 37 °C. The adenosine triphosphate concertation was measured using a CellTiter-Glo 3D Cell Viability kit (Promega) by measuring the generated chemiluminescence with an infinite M200 PRO (Tecan) plate reader.

SUPPORTING FIGURES AND TABLES

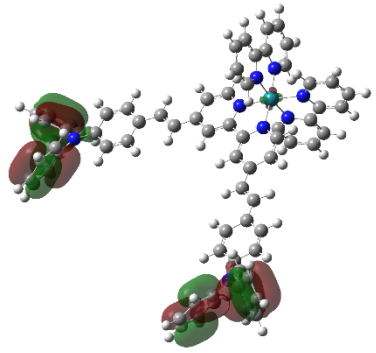	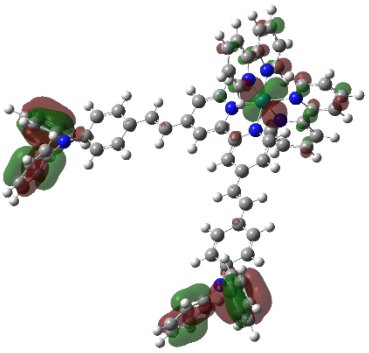	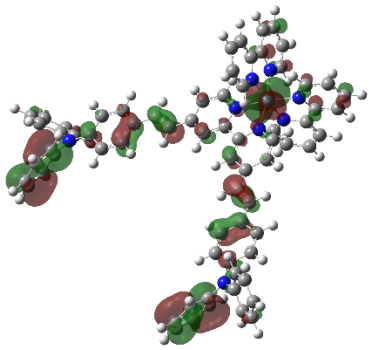
262	263	264
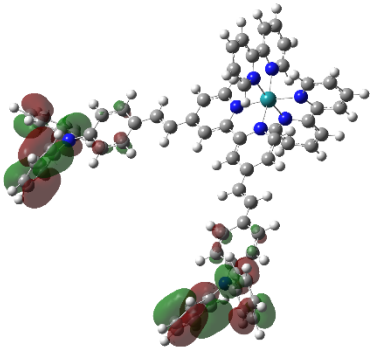	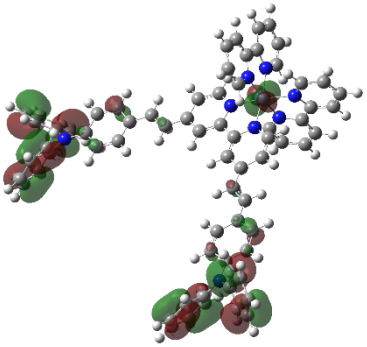	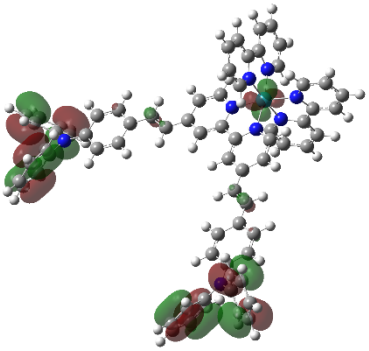
265	266	267
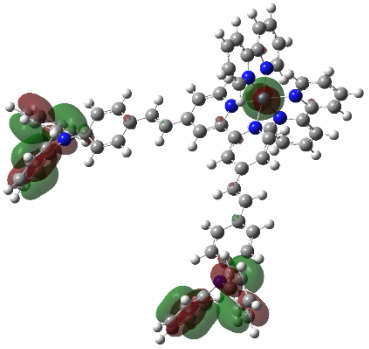	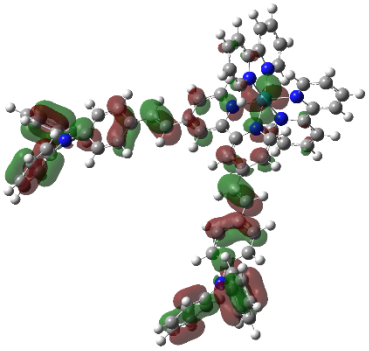	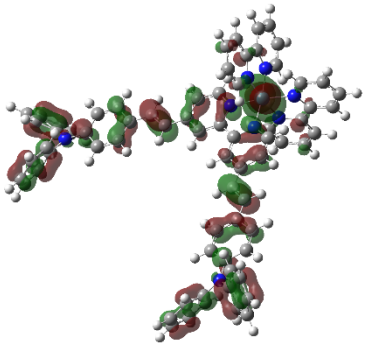
268	269	270
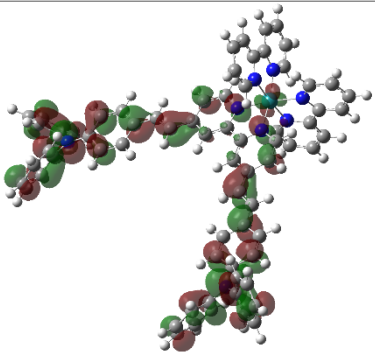	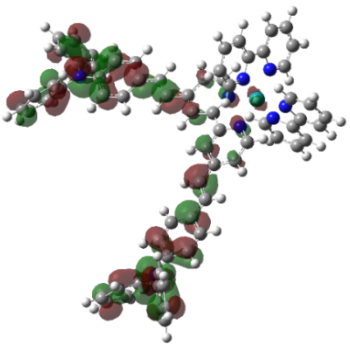	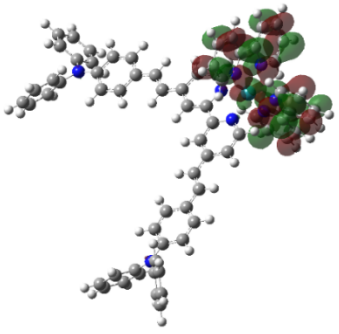
271	272 (HOMO)	273 (LUMO)

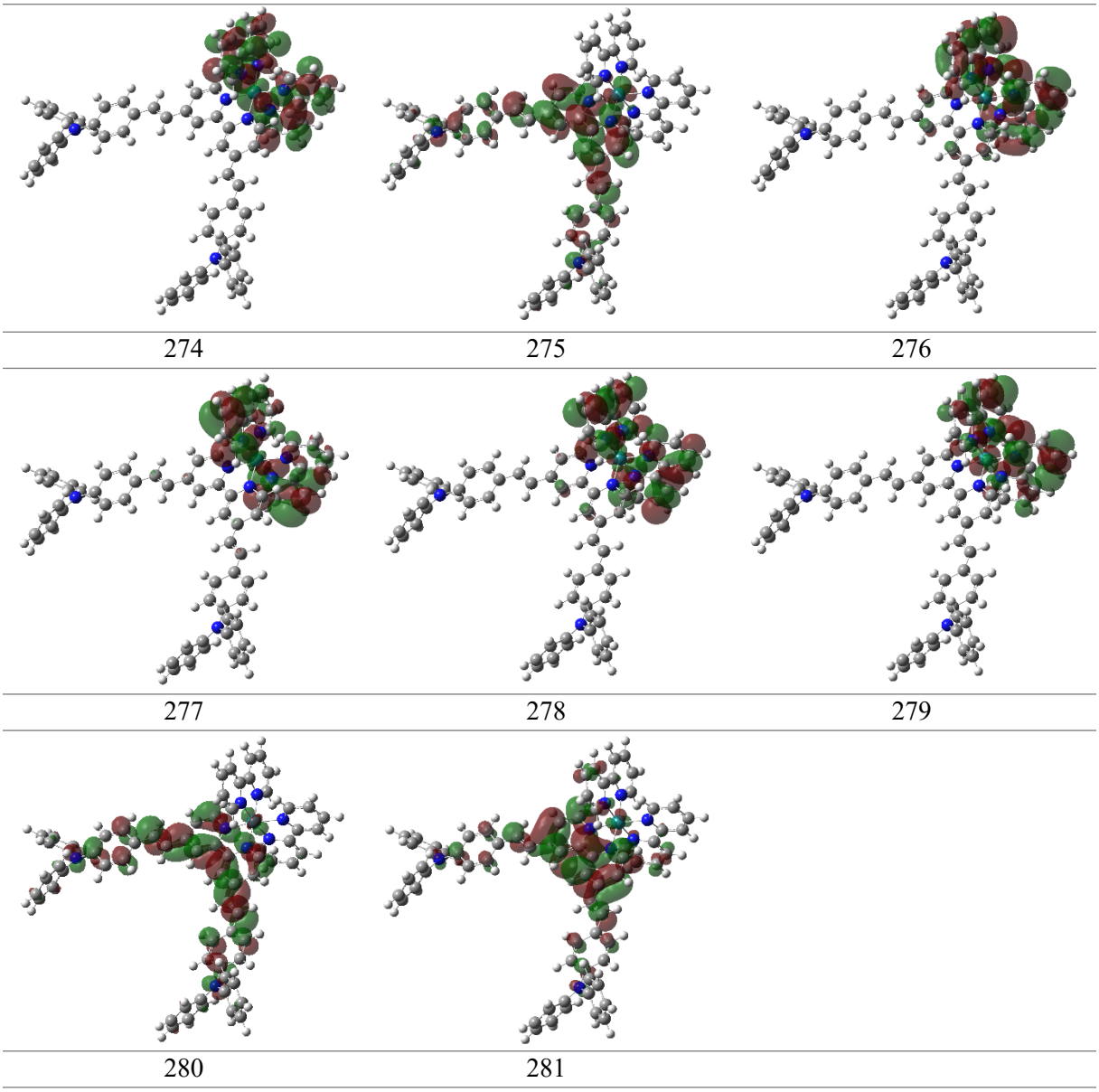

Figure S1. Computed frontier orbitals of [Ru(2,2′-bipyridine)$_2$((*E,E′*)-4,4'-bis[p-(*N,N*-phenyl-amino)styryl]-2,2'-bipyridine)].

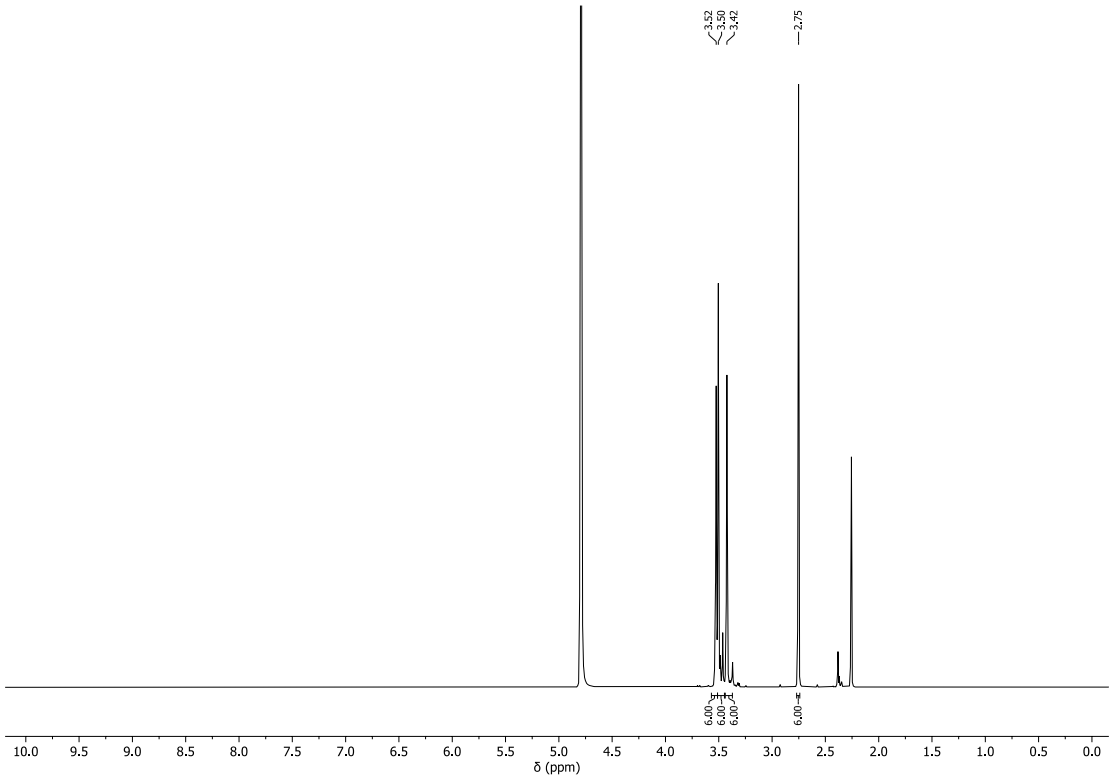

Figure S2. ^{1}H-NMR spectrum (400 MHz) of $[Ru(DMSO)_4(Cl)_2]$ in D_2O.

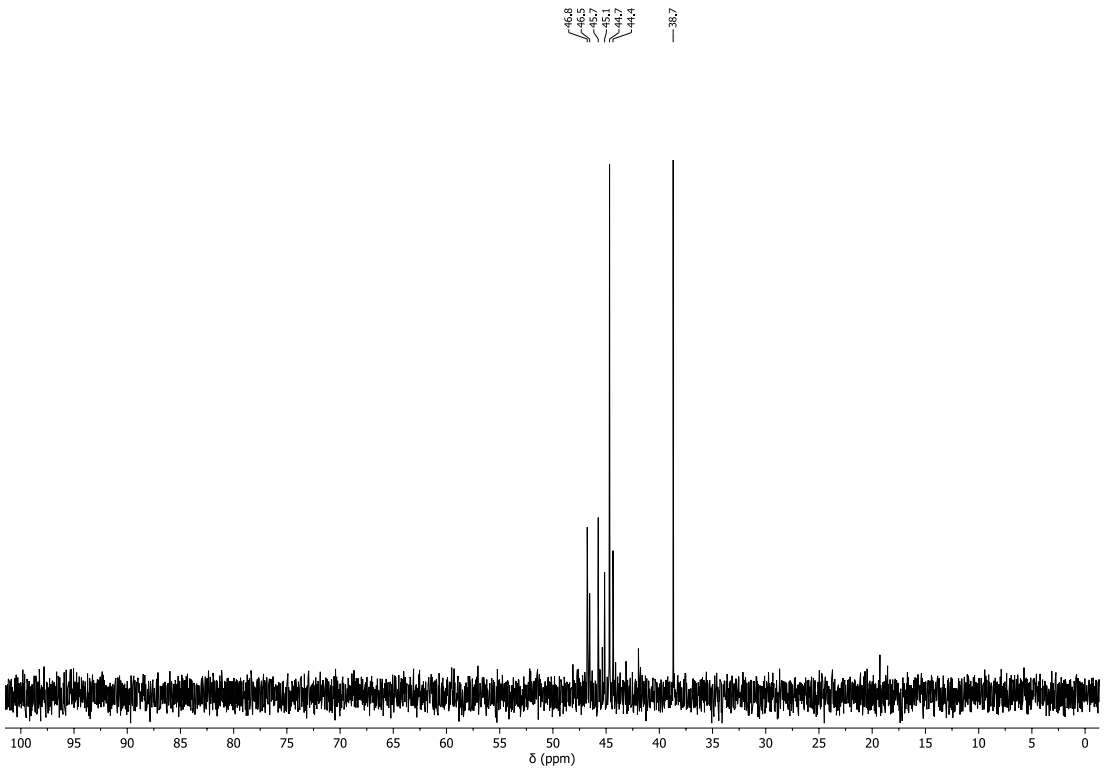

Figure S3. ^{13}C-NMR spectrum (100 MHz) of $[Ru(DMSO)_4(Cl)_2]$ in D_2O.

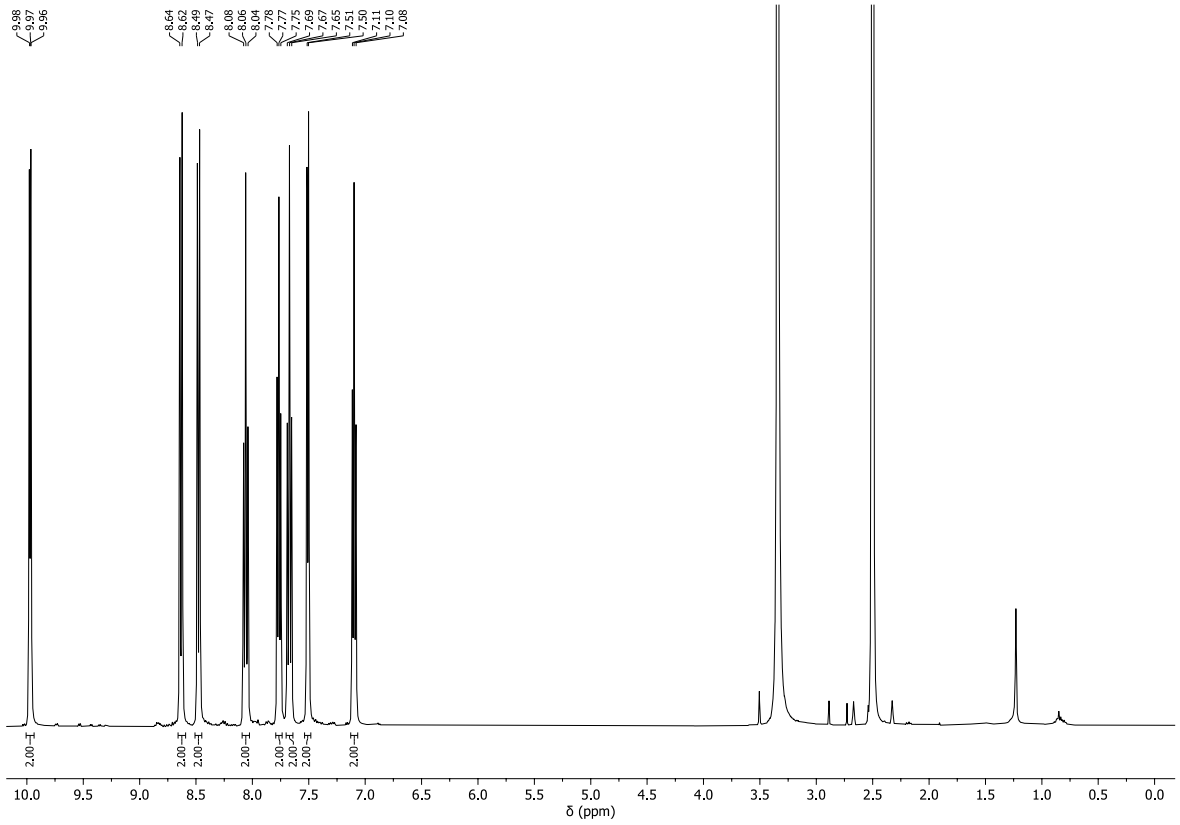

Figure S4. ^{1}H-NMR spectrum (400 MHz) of [Ru(2,2′-bipyridine)$_2$(Cl)$_2$] in DMSO-d$_6$.

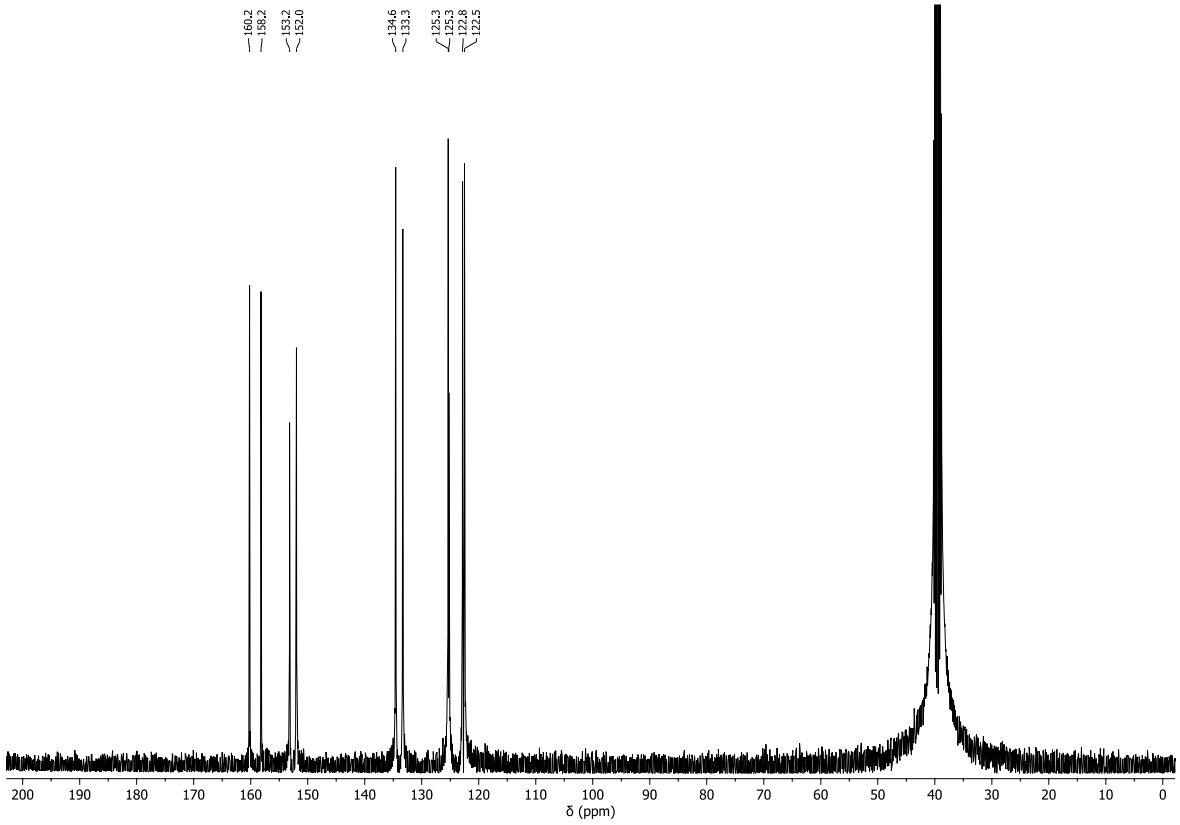

Figure S5. ^{13}C-NMR spectrum (100 MHz) of [Ru(2,2′-bipyridine)$_2$(Cl)$_2$] in DMSO-d$_6$.

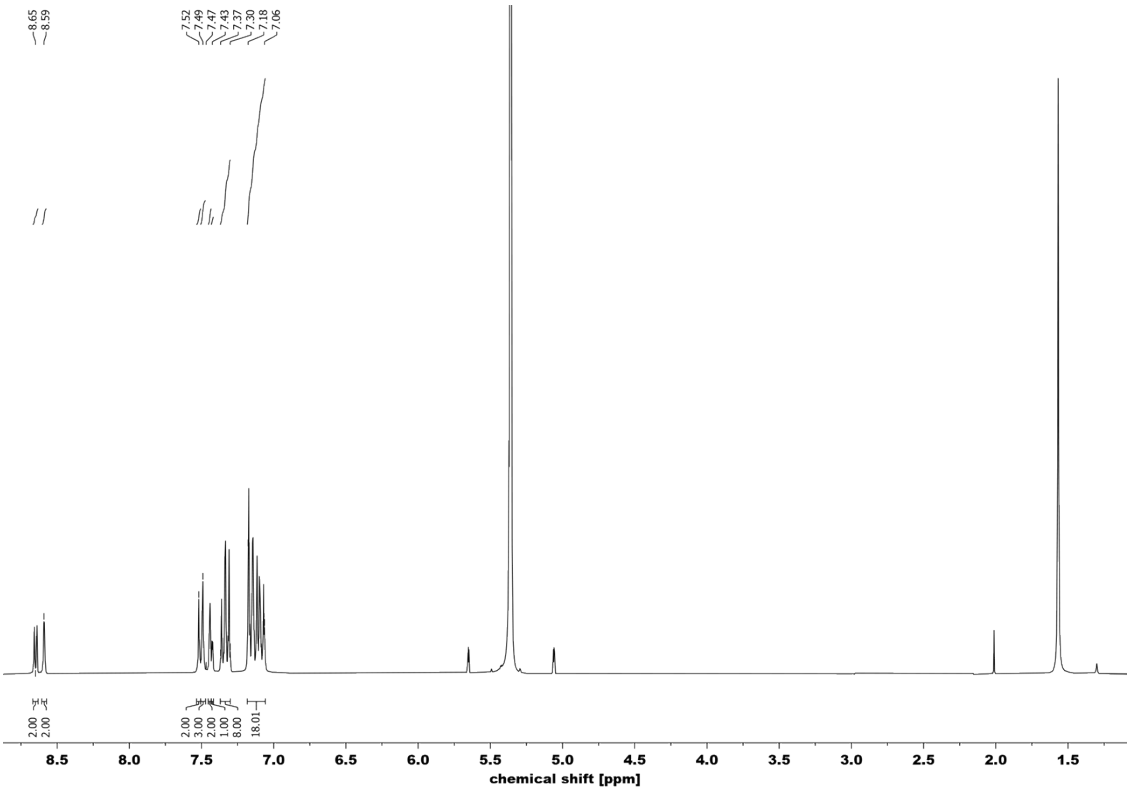

Figure S6. ^{1}H-NMR spectrum (300 MHz) of (*E, E'*)-4,4'-bis[p-(*N, N*-phenylamino)styryl]-2,2'-bipyridine in DCM-d_2.

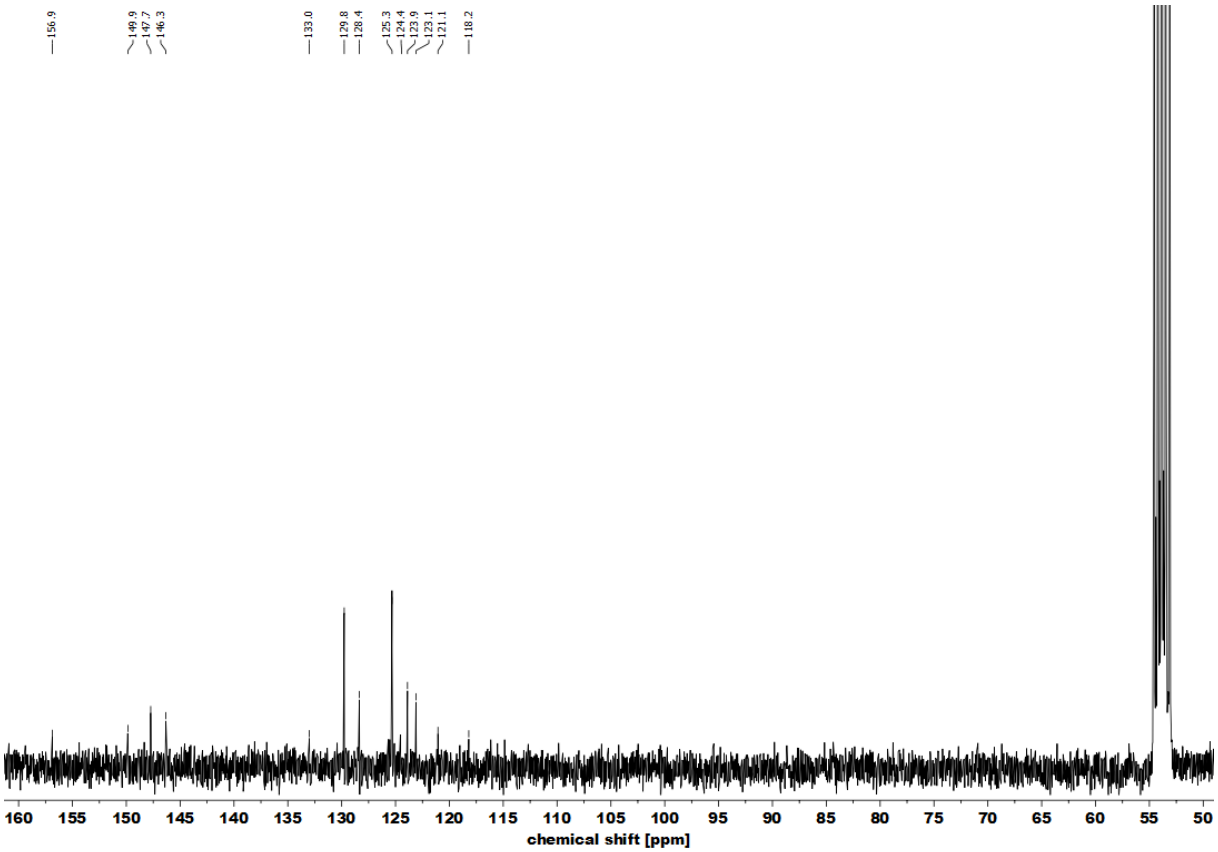

Figure S7. ^{13}C-NMR spectrum (100 MHz) of (*E, E'*)-4,4'-bis[p-(*N, N*-phenylamino)styryl]-2,2'-bipyridine in DCM-d_2.

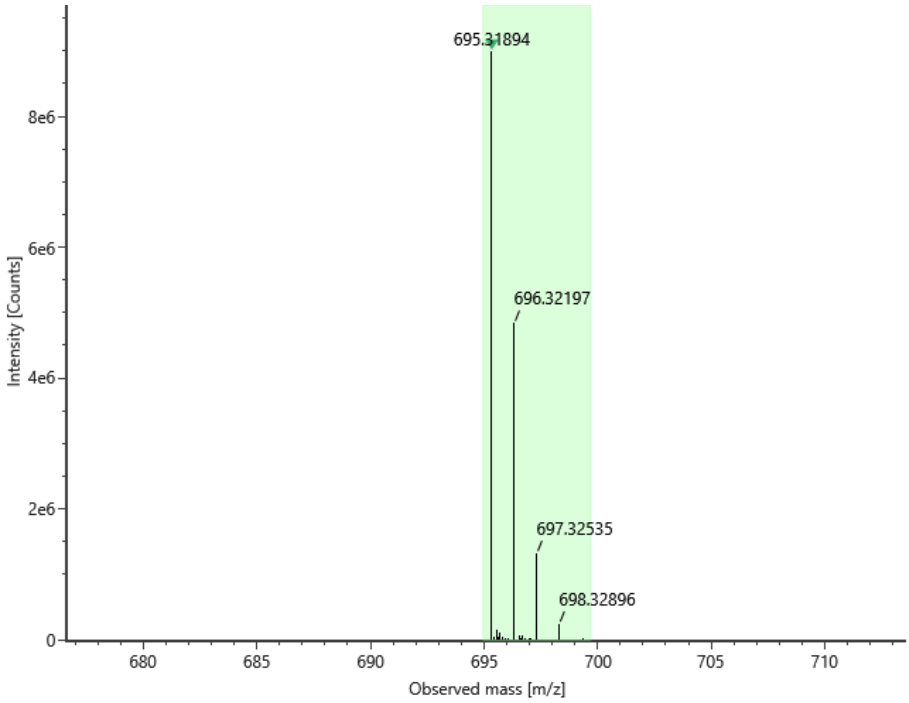

Figure S8. ESI-HRMS spectrum of (*E, E'*)-4,4'-bis[p-(*N, N*-phenylamino)styryl]-2,2'-bipyridine (positive detection mode).

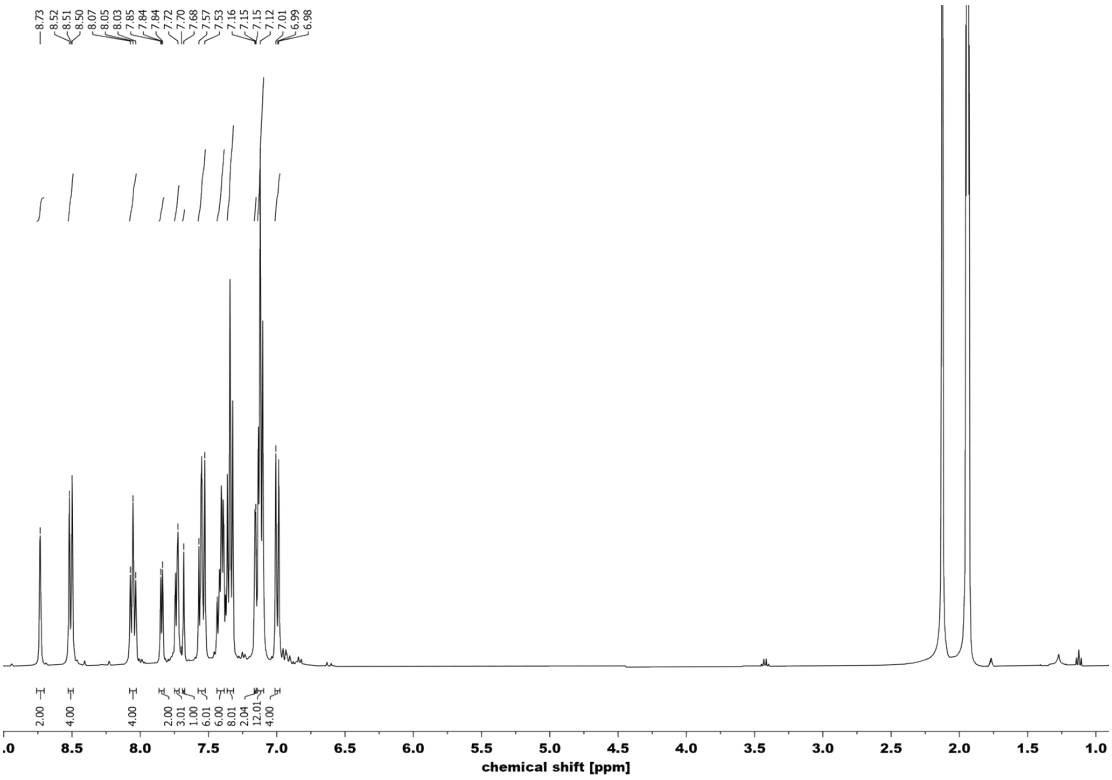

Figure S9. ^{1}H-NMR spectrum (400 MHz) of [Ru(2,2′-bipyridine)$_2$((*E,E′*)-4,4'-bis[p-(*N,N*-phenyl-amino)styryl]-2,2'-bipyridine)][PF_6]$_2$ in CD_3CN.

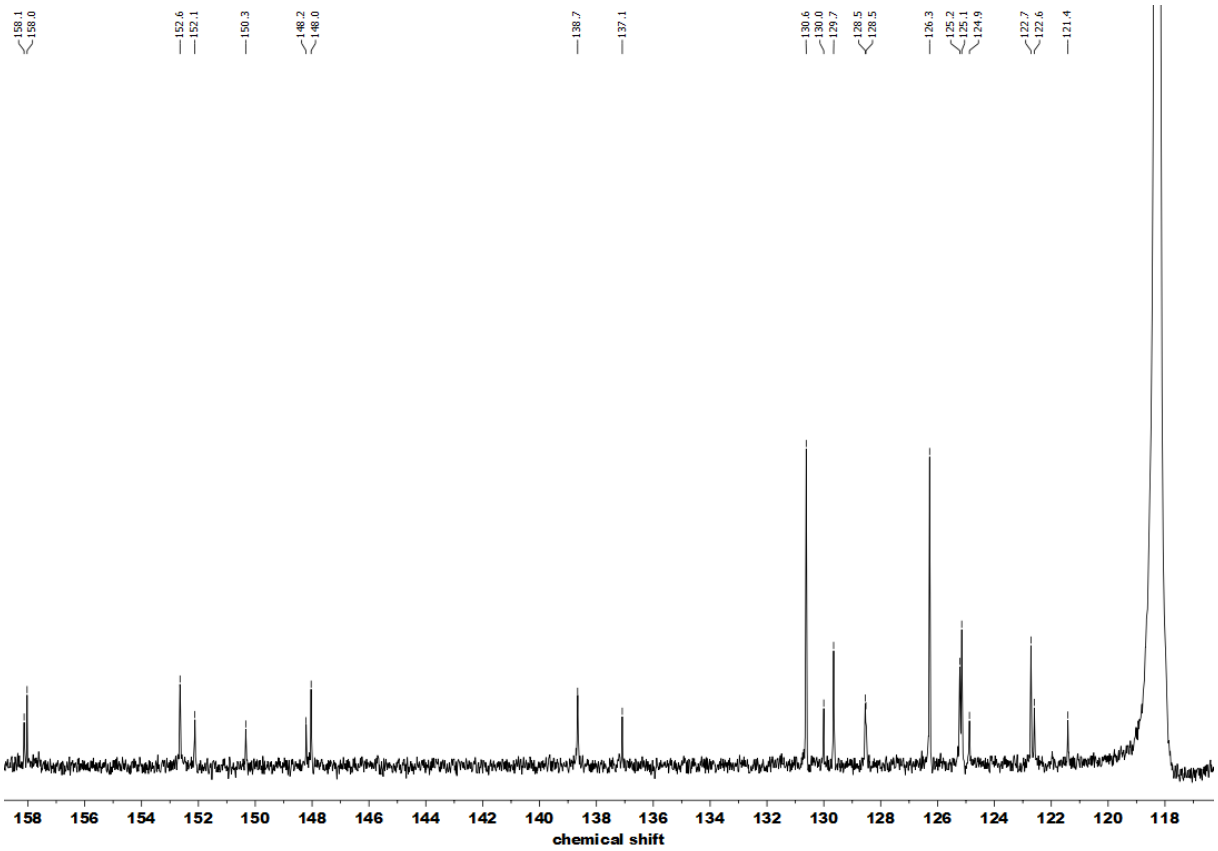

Figure S10. ^{13}C-NMR spectrum (100 MHz) of [Ru(2,2′-bipyridine)$_2$((*E,E′*)-4,4'-bis[p-(*N,N*-phenyl-amino)styryl]-2,2'-bipyridine)][PF_6]$_2$ in CD_3CN.

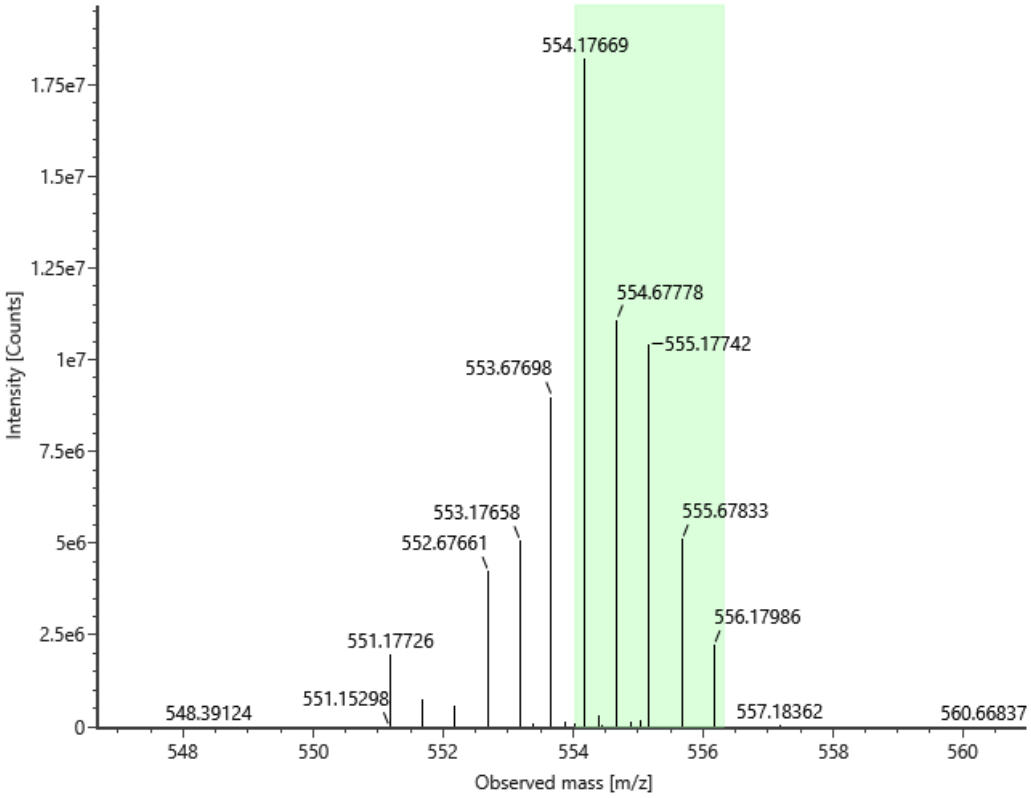

Figure S11. ESI-HRMS spectrum of [Ru(2,2′-bipyridine)$_2$((*E,E′*)-4,4'-bis[p-(*N,N*-phenyl-amino)styryl]-2,2'-bipyridine)][PF_6]$_2$ (positive detection mode).

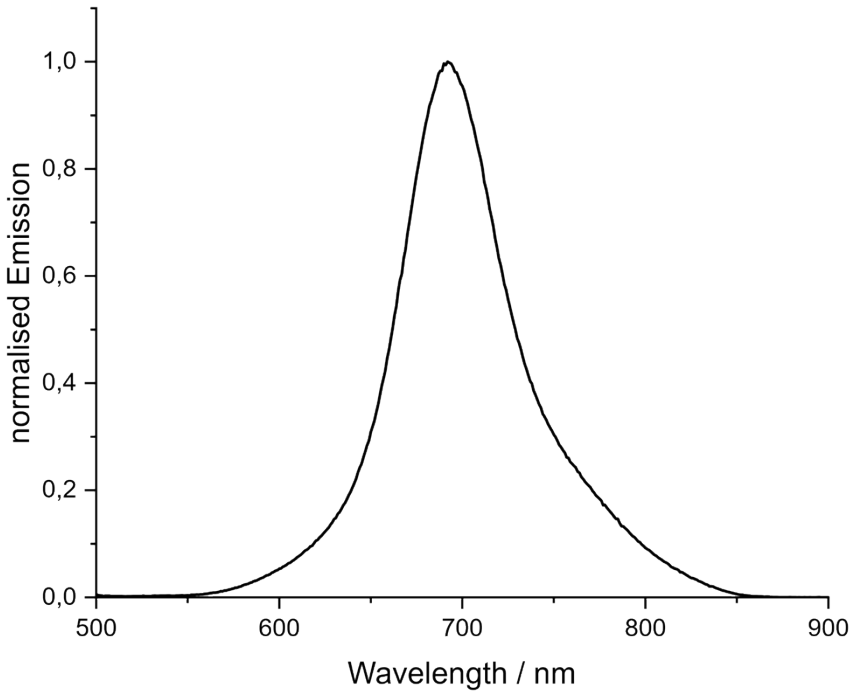

Figure S12. Emission spectrum of [Ru(2,2′-bipyridine)$_2$((*E,E′*)-4,4'-bis[p-(*N,N*-phenyl-amino)styryl]-2,2'-bipyridine)][PF_6]$_2$ in water upon excitation at 420 nm.

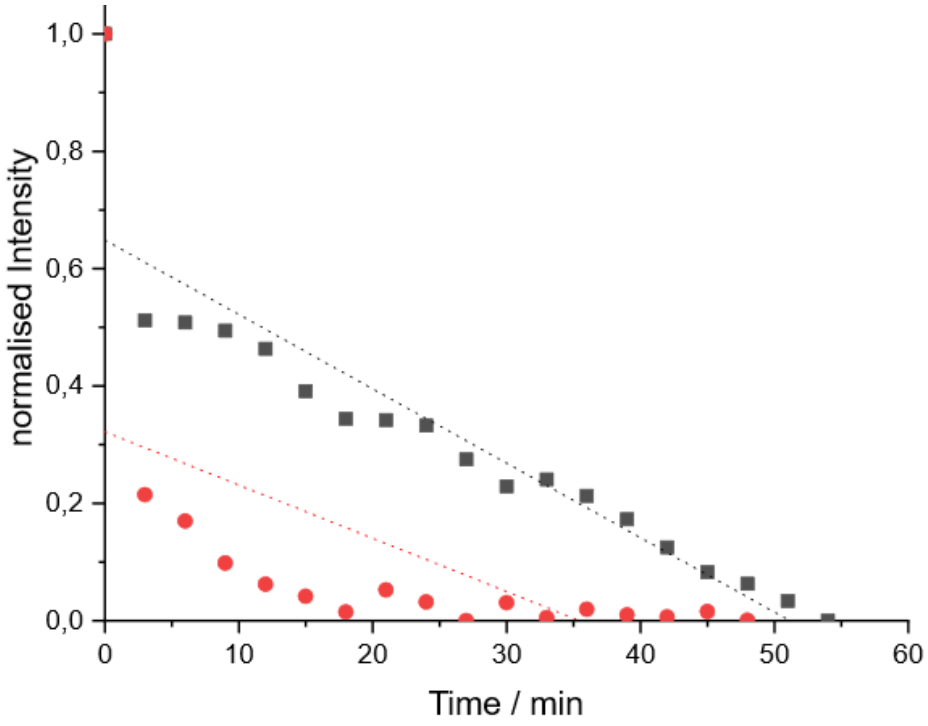

Figure S13. Linear regression of the reactive oxygen species production of [Ru(2,2′-bipyridine)$_2$((*E,E′*)-4,4'-bis[p-(*N,N*-phenyl-amino)styryl]-2,2'-bipyridine)][PF_6]$_2$ (red) in comparison to [Ru(2,2′-bipyridine)$_3$][Cl]$_2$ (black) in acetonitrile after light irradiation every 3 min with 100 µW/cm² using a 420 nm long-pass filter.

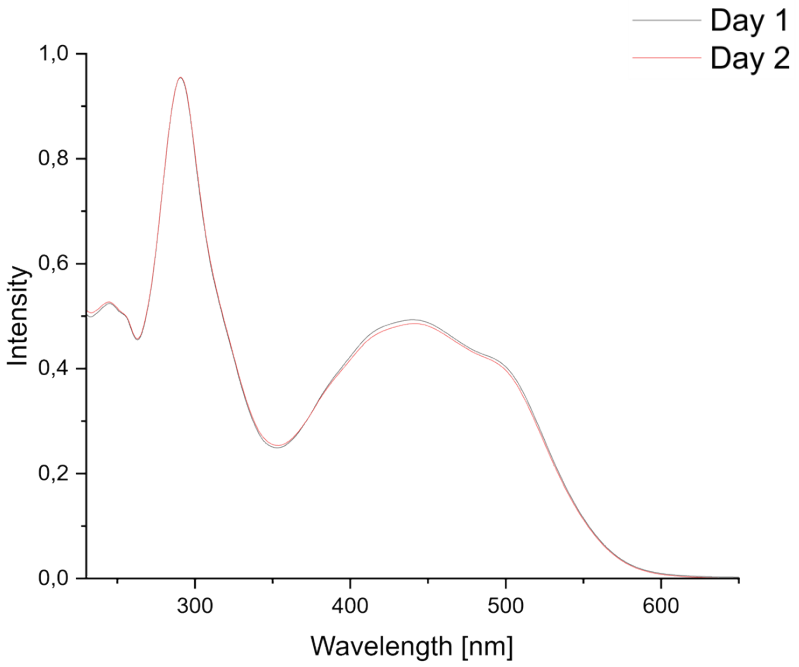

Figure S14. Temporal change of the absorption spectrum of [Ru(2,2′-bipyridine)$_2$((*E,E′*)-4,4'-bis[p-(*N,N*-phenyl-amino)styryl]-2,2'-bipyridine)][PF_6]$_2$ upon incubation in water for 1 or 2 days.

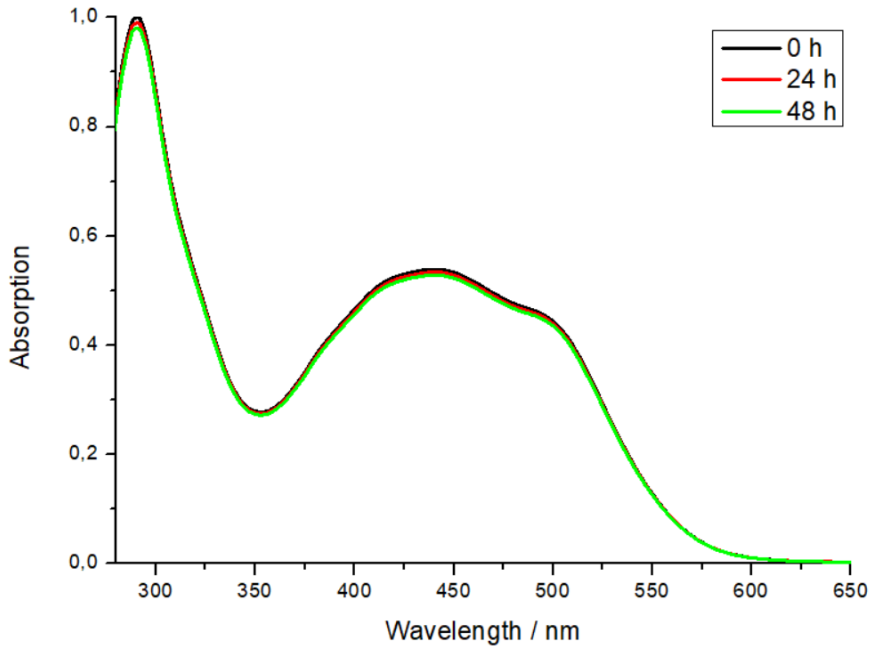

Figure S15. Temporal change of the absorption spectrum of [Ru(2,2′-bipyridine)$_2$((*E,E′*)-4,4'-bis[p-(*N,N*-phenyl-amino)styryl]-2,2'-bipyridine)][PF_6]$_2$ upon incubation in DMEM cell media for 1 or 2 days.

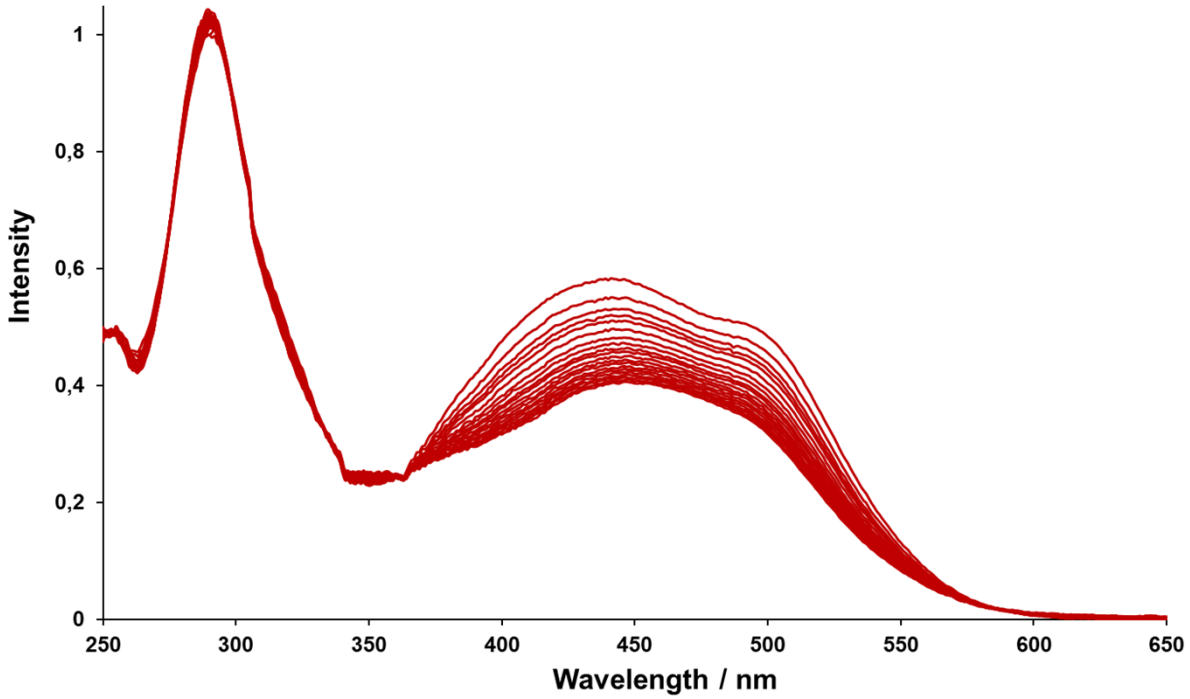

Figure S16. Temporal change of the absorption spectrum of [Ru(2,2′-bipyridine)$_2$((*E,E′*)-4,4'-bis[p-(*N,N*-phenyl-amino)styryl]-2,2'-bipyridine)][PF_6]$_2$ in water. Each measurement was done after 3 min of light irradiation, reaching a total irradiation time of 60 min with 100 µW/cm² using a 420 nm long-pass filter.

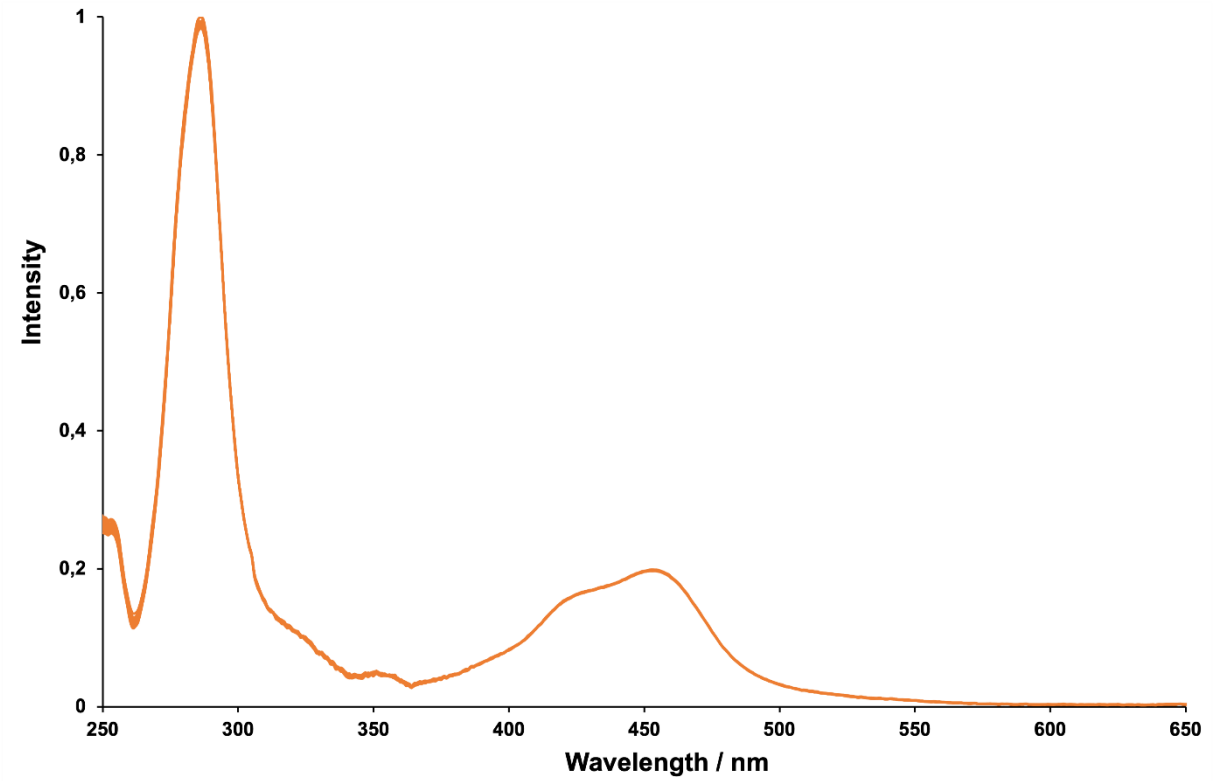

Figure S17. Temporal change of the absorption spectrum of [Ru(2,2'-bipyridine)$_3$]Cl$_2$ in water. Each measurement was done after 3 min of light irradiation, reaching a total irradiation time of 60 min with 100 μW/cm² using a 420 nm long-pass filter.

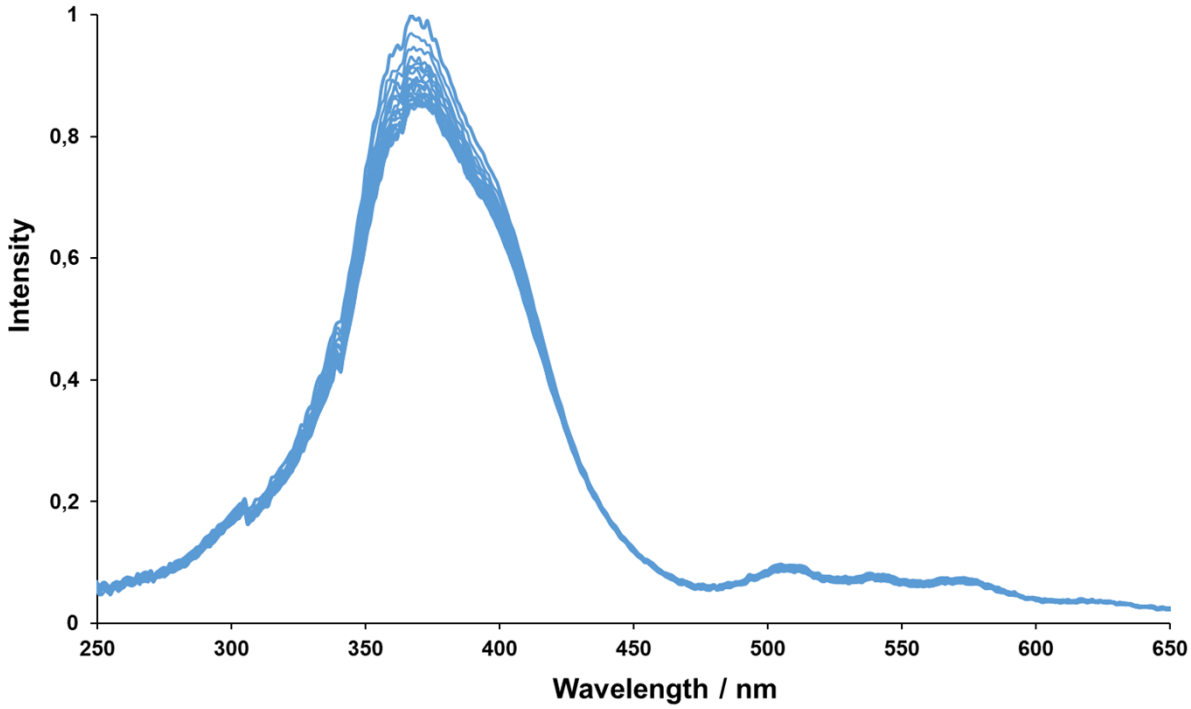

Figure S18. Temporal change of the absorption spectrum of Photofrin in water. Each measurement was done after 3 min of light irradiation, reaching a total irradiation time of 60 min with 100 μW/cm² using a 420 nm long-pass filter.

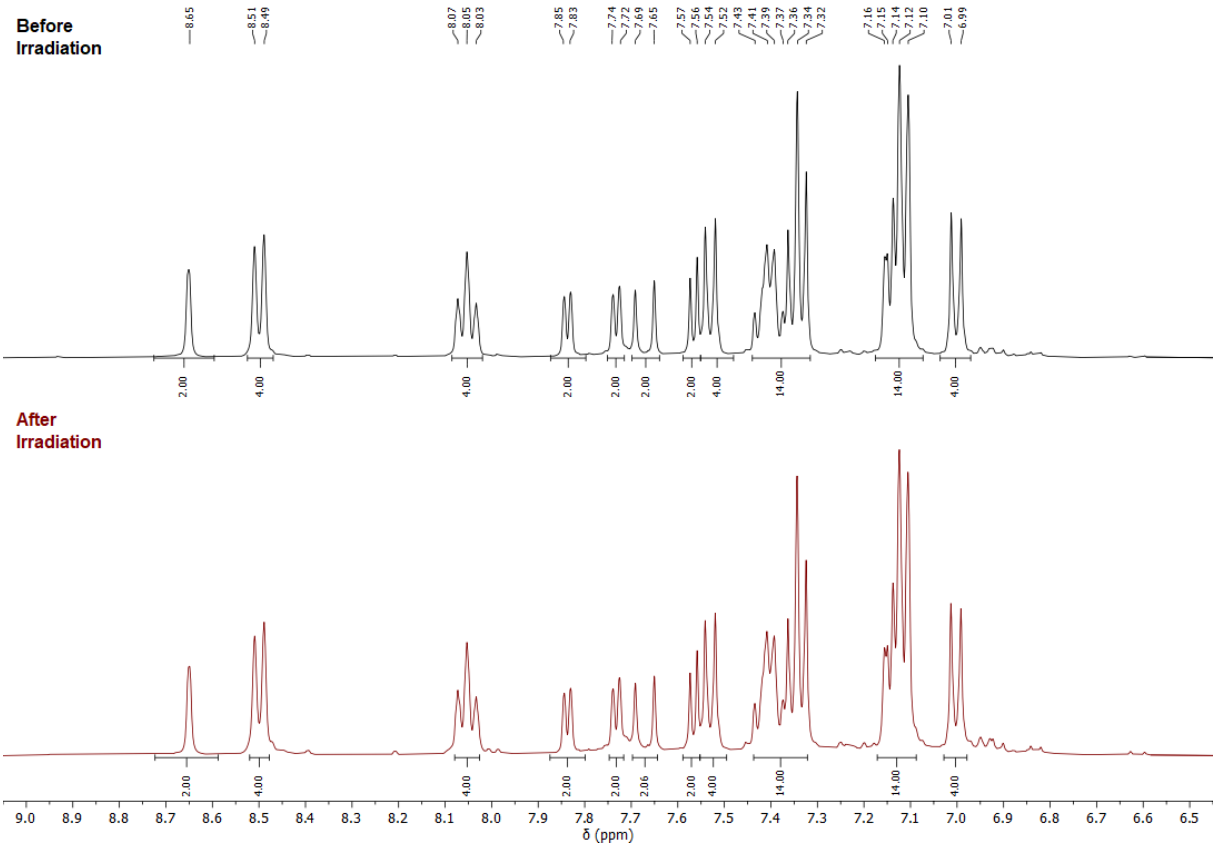

Figure S18. ^{1}H-NMR spectrum (400 MHz) of [Ru(2,2′-bipyridine)$_2$((*E,E′*)-4,4'-bis[p-(*N,N*-phenyl-amino)styryl]-2,2'-bipyridine)][PF_6]$_2$ in D_2O before and after 60 min of light irradiation.

Table S1. Computationally optimized geometry of the proposed metal complex A.

Symbol	x	y	z
C	1.057502	-1.954198	-2.131893
H	0.019578	-1.940684	-2.468736
C	2.02399	-2.74199	-2.780574
H	1.733003	-3.355963	-3.636943
C	3.356922	-2.725532	-2.307713
C	3.673921	-1.916377	-1.199098
H	4.697807	-1.89444	-0.818132
C	2.667162	-1.13964	-0.581448
C	2.888479	-0.26324	0.582333
C	4.143185	-0.058029	1.200414
H	5.033942	-0.563343	0.819392
C	4.248005	0.80397	2.309572
C	3.082544	1.450796	2.782702
H	3.117689	2.12849	3.639731
C	1.858088	1.216914	2.133465
H	0.938137	1.697329	2.470826
C	1.16724	1.893431	-2.129289
H	1.674893	0.987918	-2.465994
C	1.366531	3.12474	-2.777255
H	2.044532	3.180489	-3.632939
C	0.685	4.270324	-2.304461
C	-0.175652	4.139646	-1.197126
H	-0.707374	5.015113	-0.816682
C	-0.345512	2.878964	-0.580376
C	-1.21717	2.631581	0.581685
C	-2.02368	3.615215	1.198547
H	-2.031555	4.639305	0.817629
C	-2.823974	3.274529	2.306426
C	-2.801599	1.9419	2.779682
H	-3.407296	1.633412	3.635802
C	-1.985735	0.998607	2.131391

H	-1.941895	-0.03842	2.46846
C	-2.219037	0.06356	-2.133471
H	-1.687041	0.954863	-2.470393
C	-3.384933	-0.378091	-2.782467
H	-3.77009	0.181215	-3.639107
C	-4.039143	-1.539365	-2.309329
C	-3.498169	-2.219189	-1.200568
H	-3.992635	-3.116006	-0.819513
C	-2.321357	-1.737541	-0.582937
C	-1.673288	-2.368953	0.58012
C	-2.124423	-3.557776	1.197747
H	-3.00884	-4.074629	0.817436
C	-1.43024	-4.08168	2.305807
C	-0.285553	-3.398316	2.778294
H	0.283938	-3.769284	3.634486
C	0.125593	-2.221128	2.129614
H	1.002768	-1.666139	2.466549
N	1.358749	-1.161021	-1.0529
N	1.747026	0.376754	1.053718
N	0.328452	1.757211	-1.051454
N	-1.201319	1.323018	1.052816
N	-1.684092	-0.594526	-1.054131
N	-0.546699	-1.702778	1.050971
Ru	0.000541	-0.000293	0.000116
H	-4.949503	-1.904376	-2.792711
H	-1.771976	-5.000839	2.789551
H	4.129175	-3.330117	-2.791189
H	5.214568	0.96904	2.793465
H	-3.4514	4.028824	2.789343
H	0.822785	5.241756	-2.787336

Table S2. Computationally optimized geometry of the proposed metal complex B.

Symbol	x	y	z
C	2.645711	-1.518651	1.571218
H	2.354323	-0.837996	2.37306
C	3.66403	-2.469411	1.756055
H	4.17827	-2.528501	2.718917
C	4.00511	-3.330738	0.687098
C	3.309845	-3.207952	-0.531639
H	3.562794	-3.862228	-1.369473
C	2.291403	-2.237108	-0.668518
C	1.506265	-2.021324	-1.89626
C	1.644725	-2.78506	-3.07768
H	2.370629	-3.60049	-3.124063
C	0.84206	-2.497651	-4.198836
C	-0.094084	-1.44072	-4.113511
H	-0.738579	-1.183781	-4.95828
C	-0.197158	-0.711407	-2.916596
H	-0.907807	0.110185	-2.812632
C	-1.041095	-2.493724	0.999927
H	-0.033597	-2.879076	1.166944
C	-2.165665	-3.272016	1.291608
H	-2.016636	-4.279451	1.688897
C	-3.47681	-2.753678	1.068502
C	-3.553117	-1.433204	0.548019
H	-4.537728	-0.99592	0.358429
C	-2.391748	-0.685623	0.271364
C	-2.39141	0.687227	-0.270483
C	-3.552429	1.435426	-0.546987
H	-4.537225	0.998594	-0.35732
C	-3.475479	2.755922	-1.067295
C	-2.16408	3.273625	-1.290453
H	-2.014569	4.281039	-1.687629
C	-1.03989	2.494749	-0.998935

H	-0.032197	2.879564	-1.165989
C	-0.194877	0.711827	2.916963
H	-0.906457	-0.108991	2.813262
C	-0.090338	1.440824	4.113938
H	-0.734613	1.184419	4.959036
C	0.84696	2.496766	4.198905
C	1.649228	2.78357	3.077312
H	2.375992	3.598255	3.123387
C	1.509264	2.020204	1.895833
C	2.293754	2.235466	0.667597
C	3.312982	3.205397	0.530123
H	3.56715	3.859288	1.36789
C	4.007437	3.327766	-0.689117
C	3.664748	2.466954	-1.757976
H	4.178303	2.525759	-2.72122
C	2.645702	1.517091	-1.572545
H	2.353085	0.836839	-2.374281
N	1.96145	-1.394116	0.387654
N	0.5836	-0.982986	-1.820548
N	-1.127098	-1.215769	0.498956
N	-1.126513	1.216728	-0.498141
N	0.585531	0.982774	1.820501
N	1.962233	1.392951	-0.388475
Ru	0.476475	-0.000006	0.000016
H	0.947966	3.082414	5.11675
H	4.797955	4.074448	-0.80399
H	4.795026	-4.078127	0.801509
H	0.941903	-3.083582	-5.116628
C	-4.714008	3.501125	-1.34141
H	-5.646831	2.968116	-1.113862
C	-4.798923	4.765902	-1.841159
H	-5.772481	5.235749	-2.010108
H	-3.922435	5.372699	-2.096949

C	-4.715736	-3.498245	1.342677
H	-5.648304	-2.964628	1.115567
C	-4.801244	-4.763091	1.842165
H	-3.925043	-5.370402	2.097707
H	-5.775001	-5.232436	2.011319

Table S3. Computationally optimized geometry of the proposed metal complex C.

Symbol	**x**	**y**	**z**
C	-1.940219	-4.111479	0.992863
H	-1.543575	-3.830556	1.970135
C	-2.906626	-5.122703	0.860227
H	-3.267585	-5.643693	1.750937
C	-3.391921	-5.447975	-0.428381
C	-2.887906	-4.745812	-1.540165
H	-3.246893	-4.986792	-2.543755
C	-1.916059	-3.735674	-1.355948
C	-1.314908	-2.948643	-2.445677
C	-1.662673	-3.075992	-3.809877
H	-2.428283	-3.792459	-4.117615
C	-1.023803	-2.274929	-4.776017
C	-0.039395	-1.351718	-4.351712
H	0.480784	-0.708355	-5.06626
C	0.270338	-1.258655	-2.984339
H	1.021686	-0.557271	-2.617952
C	-2.683589	-0.41504	0.16512
H	-3.103763	-1.422194	0.199513
C	-3.513461	0.706522	0.202419
H	-4.593286	0.549363	0.263675
C	-2.955938	2.026608	0.156978
C	-1.531823	2.092735	0.074954
H	-1.052912	3.075454	0.03448
C	-0.737672	0.933806	0.042545
C	0.737828	0.933672	-0.042654
C	1.532191	2.092456	-0.075058
H	1.053461	3.075262	-0.034561
C	2.956293	2.026067	-0.157115
C	3.513569	0.705881	-0.202596
H	4.593363	0.548523	-0.263889
C	2.683491	-0.41553	-0.165297

H	3.103485	-1.422757	-0.199729
C	-0.270614	-1.258309	2.984275
H	-1.021892	-0.556882	2.617834
C	0.039139	-1.35126	4.351653
H	-0.480954	-0.707764	5.066142
C	1.023451	-2.274538	4.776033
C	1.662205	-3.075781	3.809965
H	2.427731	-3.792307	4.117766
C	1.31442	-2.948539	2.445759
C	1.91544	-3.735787	1.356112
C	2.887168	-4.746022	1.540436
H	3.246166	-4.986903	2.544044
C	3.39105	-5.448408	0.428733
C	2.905743	-5.123267	-0.859902
H	3.266595	-5.644434	-1.750551
C	1.939462	-4.111937	-0.992645
H	1.542811	-3.831107	-1.969943
N	-1.446405	-3.419102	-0.085068
N	-0.34555	-2.037922	-2.03611
N	-1.311534	-0.332934	0.090124
N	1.311457	-0.333174	-0.090257
N	0.345166	-2.037746	2.036117
N	1.445783	-3.419333	0.085204
Ru	-0.000191	-1.939379	-0.000009
H	1.28651	-2.365435	5.833459
H	4.141852	-6.232095	0.562131
H	-4.142815	-6.231589	-0.561694
H	-1.286848	-2.365908	-5.833438
C	3.734907	3.25447	-0.188717
H	3.152137	4.183259	-0.14219
C	5.109566	3.332546	-0.270542
H	5.684802	2.395759	-0.317625
C	-3.734321	3.255158	0.188609

H	-3.151367	4.18383	0.142114
C	-5.108966	3.333489	0.270423
H	-5.684373	2.3968	0.317436
C	-5.924963	4.544013	0.304204
C	-5.376792	5.863014	0.251724
C	-7.343385	4.400718	0.39437
C	-6.218578	6.987658	0.288533
H	-4.293691	6.010917	0.18182
C	-8.184982	5.528488	0.431209
H	-7.780434	3.395221	0.435486
C	-7.62503	6.826521	0.378417
H	-5.789298	7.993962	0.247655
H	-9.269874	5.401965	0.50051
H	-8.27576	7.706604	0.406755
C	5.925767	4.542928	-0.304289
C	7.344157	4.399408	-0.3946
C	5.377819	5.862018	-0.251648
C	8.185937	5.52704	-0.431423
H	7.781033	3.39384	-0.435841
C	6.219787	6.986525	-0.288449
H	4.294749	6.010092	-0.181605
C	7.626204	6.825162	-0.378479
H	9.270802	5.400346	-0.500832
H	5.790677	7.992897	-0.24745
H	8.277082	7.705136	-0.406807

Table S4. Computationally optimized geometry of the proposed metal complex D.

Symbol	x	y	z
C	-1.963169	4.428326	-0.935106
H	-1.581825	4.158785	-1.921728
C	-2.933707	5.431104	-0.775314
H	-3.313582	5.958583	-1.654294
C	-3.399682	5.739255	0.525001
C	-2.870739	5.030281	1.620405
H	-3.213272	5.258157	2.632829
C	-1.894235	4.029727	1.409258
C	-1.262784	3.241094	2.479299
C	-1.580028	3.356411	3.852017
H	-2.346505	4.062504	4.181104
C	-0.910112	2.557152	4.797999
C	0.07476	1.647917	4.344459
H	0.618411	1.005518	5.042249
C	0.353753	1.565885	2.970176
H	1.102397	0.874189	2.580786
C	-2.687701	0.726325	-0.12222
H	-3.108839	1.733669	-0.146503
C	-3.517599	-0.392938	-0.152228
H	-4.598012	-0.234105	-0.197259
C	-2.961194	-1.718515	-0.11993
C	-1.532193	-1.780091	-0.057866
H	-1.051038	-2.762274	-0.028363
C	-0.738504	-0.623074	-0.032023
C	0.738477	-0.623112	0.03195
C	1.532101	-1.780178	0.057799
H	1.050883	-2.76233	0.028318
C	2.961104	-1.718682	0.119838
C	3.517586	-0.393135	0.152098
H	4.598009	-0.234362	0.197086
C	2.687754	0.726174	0.122091

H	3.108941	1.733498	0.146333
C	-0.353601	1.566075	-2.970217
H	-1.102247	0.874359	-2.580869
C	-0.074598	1.648185	-4.344493
H	-0.618245	1.005826	-5.042324
C	0.91028	2.557444	-4.797975
C	1.580194	3.356645	-3.851944
H	2.34668	4.06275	-4.180984
C	1.26294	3.241251	-2.479234
C	1.894401	4.029803	-1.40914
C	2.870884	5.03039	-1.620222
H	3.213378	5.25837	-2.632635
C	3.399852	5.739266	-0.524766
C	2.933926	5.430981	0.775533
H	3.313827	5.958375	1.654553
C	1.963401	4.428179	0.93526
H	1.582091	4.158541	1.921868
N	-1.445753	3.727852	0.126781
N	-0.293013	2.343499	2.040588
N	-1.313176	0.645917	-0.067432
N	1.313218	0.645842	0.067339
N	0.293162	2.343635	-2.04058
N	1.445951	3.727808	-0.126679
Ru	0.000072	2.253557	-0.000002
H	1.149782	2.638767	-5.861761
H	4.154593	6.515352	-0.678893
H	-4.154441	6.515313	0.679177
H	-1.149606	2.638418	5.861792
C	3.736425	-2.939804	0.145818
H	3.155352	-3.870424	0.112114
C	5.120328	-3.015257	0.208413
H	5.686467	-2.072425	0.242148
C	-3.736581	-2.939591	-0.145887

H	-3.155575	-3.870249	-0.112064
C	-5.120493	-3.014969	-0.208575
H	-5.686576	-2.072109	-0.242454
C	-5.940273	-4.206014	-0.236402
C	-7.365458	-4.067558	-0.304859
C	-5.412248	-5.539273	-0.199457
C	-8.216131	-5.174041	-0.335188
H	-7.80061	-3.060908	-0.334366
C	-6.247851	-6.655261	-0.228903
H	-4.329872	-5.698385	-0.146541
C	-7.673333	-6.49859	-0.297721
H	-9.301679	-5.03462	-0.387705
H	-5.820019	-7.664067	-0.199423
C	5.940044	-4.206339	0.236307
C	7.365251	-4.067936	0.304511
C	5.411954	-5.539573	0.199642
C	8.215878	-5.174451	0.334884
H	7.800444	-3.061297	0.333781
C	6.247511	-6.655597	0.229127
H	4.329565	-5.698651	0.146905
C	7.67301	-6.49898	0.297708
H	9.30144	-5.035068	0.387203
H	5.819634	-7.664389	0.199854
N	8.49829	-7.602166	0.326893
H	9.510301	-7.501889	0.375442
H	8.118788	-8.546449	0.300572
N	-8.498666	-7.601743	-0.326841
H	-9.510664	-7.501422	-0.37556
H	-8.119211	-8.54604	-0.30032

Table S5. Computationally optimized geometry of the proposed metal complex E.

Symbol	**x**	**y**	**z**
C	2.402903	-5.86325	-0.900096
H	2.018193	-5.610732	-1.889925
C	3.402516	-6.835204	-0.730178
H	3.802183	-7.355946	-1.60439
C	3.871884	-7.121502	0.574026
C	3.316534	-6.422884	1.662894
H	3.66115	-6.634394	2.67817
C	2.310834	-5.453817	1.441717
C	1.64955	-4.679977	2.504159
C	1.961625	-4.779547	3.879344
H	2.747427	-5.460357	4.216086
C	1.261631	-3.997336	4.817621
C	0.25189	-3.120888	4.353922
H	-0.315535	-2.492408	5.045441
C	-0.021125	-3.053407	2.977758
H	-0.788089	-2.386631	2.580612
C	3.015865	-2.138909	-0.104858
H	3.465849	-3.133897	-0.121037
C	3.81325	-0.99677	-0.139321
H	4.897953	-1.124529	-0.179501
C	3.218538	0.312969	-0.117593
C	1.788187	0.333709	-0.060262
H	1.278902	1.301872	-0.038739
C	1.02767	-0.845253	-0.029977
C	-0.448403	-0.887403	0.0286
C	-1.275336	0.246157	0.045748
H	-0.822374	1.241594	0.012836
C	-2.702241	0.144037	0.102984
C	-3.220704	-1.197429	0.140504
H	-4.296266	-1.386803	0.18322
C	-2.359007	-2.29218	0.118913

H	-2.750978	-3.311168	0.147069
C	0.725404	-3.056762	-2.956963
H	1.453227	-2.344225	-2.565741
C	0.456382	-3.150832	-4.332344
H	0.986817	-2.496577	-5.029297
C	-0.501821	-4.087186	-4.78823
C	-1.155849	-4.900397	-3.843166
H	-1.901656	-5.627574	-4.173857
C	-0.849639	-4.77205	-2.469046
C	-1.465442	-5.573653	-1.399922
C	-2.414239	-6.600317	-1.61251
H	-2.746499	-6.839352	-2.625796
C	-2.928531	-7.320618	-0.517627
C	-2.475881	-6.997428	0.78387
H	-2.844965	-7.532961	1.66258
C	-1.533294	-5.968683	0.945153
H	-1.163362	-5.686646	1.932642
N	1.859646	-5.172592	0.155365
N	0.655153	-3.814603	2.055417
N	1.639088	-2.097921	-0.055625
N	-0.986818	-2.172778	0.068259
N	0.093898	-3.847773	-2.02801
N	-1.030663	-5.256693	-0.116252
Ru	0.372227	-3.7419	0.013325
H	-0.733076	-4.178301	-5.853049
H	-3.661891	-8.116715	-0.672931
H	4.64934	-7.873189	0.736002
H	1.496947	-4.066521	5.8832
C	-3.512692	1.341571	0.119683
H	-2.958919	2.288772	0.085754
C	-4.899196	1.377432	0.172927
H	-5.438913	0.419275	0.20502
C	3.958981	1.554859	-0.149334

H	3.352248	2.46916	-0.119489
C	5.340691	1.669235	-0.212565
H	5.933843	0.742946	-0.238058
C	6.124654	2.883507	-0.251981
C	7.554055	2.78848	-0.308302
C	5.55935	4.201377	-0.253894
C	8.365313	3.922483	-0.346284
H	8.022543	1.796678	-0.315857
C	6.357053	5.345815	-0.287409
H	4.471342	4.328647	-0.24587
C	7.787284	5.233838	-0.32741
H	9.456099	3.814949	-0.380787
H	5.890716	6.333275	-0.324687
C	-5.750816	2.545467	0.193226
C	-7.171665	2.371915	0.259475
C	-5.260105	3.89345	0.163188
C	-8.057756	3.451687	0.277906
H	-7.578993	1.35435	0.310303
C	-6.130417	4.981188	0.185006
H	-4.182874	4.085208	0.117318
C	-7.55388	4.791025	0.234888
H	-9.132101	3.274403	0.363825
H	-5.729609	6.001919	0.153383
N	-8.367536	5.914901	0.277077
H	-7.891634	6.804188	0.451295
N	8.631664	6.334005	-0.392253
H	9.606318	6.133912	-0.632746
C	8.328801	7.716765	-0.189306
C	7.405489	8.148199	0.799185
C	9.039033	8.676754	-0.956902
C	7.181178	9.527776	0.990285
H	6.905183	7.418983	1.443637
C	8.816357	10.053084	-0.747526

H	9.751393	8.345381	-1.72192
C	7.879914	10.485885	0.219885
H	6.475185	9.855341	1.760839
H	9.368985	10.786486	-1.343635
H	7.707042	11.554752	0.379553
C	-9.788845	6.004768	0.142354
C	-10.470371	6.995559	0.896617
C	-10.512068	5.190485	-0.768289
C	-11.863281	7.158983	0.752048
H	-9.913762	7.623626	1.602563
C	-11.90745	5.354451	-0.89471
H	-9.98742	4.470636	-1.403706
C	-12.590451	6.333581	-0.136754
H	-12.38118	7.925028	1.338197
H	-12.459417	4.729061	-1.604314
H	-13.672217	6.459437	-0.245107

Table S6. Computationally optimized geometry of the proposed metal complex **4**.

Symbol	x	y	z
Ru	0.000013	4.736118	0.000016
N	1.439241	6.208001	-0.201522
C	1.827526	6.503624	-1.505247
C	2.008894	6.910835	0.831885
C	2.798071	7.49855	-1.765943
C	2.974903	7.908541	0.622551
H	1.673445	6.646305	1.836421
C	3.381228	8.209028	-0.699707
H	3.093669	7.720539	-2.794371
H	3.3978	8.437846	1.480546
H	4.131872	8.980498	-0.892287
N	-0.188531	4.82492	2.051685
C	0.509021	4.050351	2.946913
C	-1.140096	5.716825	2.540408
C	0.299279	4.129629	4.333337
H	1.240166	3.362708	2.519042
C	-1.387757	5.829207	3.927752
C	-0.666619	5.033025	4.837581
H	0.880773	3.489104	5.001739
H	-2.140491	6.530931	4.295699
H	-0.852477	5.111794	5.912233
N	-1.314854	3.129447	-0.006172
C	-0.738576	1.85923	0.001841
C	-2.691171	3.209452	0.000755
C	-1.533239	0.702825	0.011117
C	-3.521468	2.090936	0.00673
H	-3.112759	4.216979	-0.003227
C	-2.963704	0.764019	0.0133
H	-1.051169	-0.279439	0.018083
H	-4.602857	2.249336	0.011467
N	-1.439248	6.207984	0.201435

C	-1.827533	6.503703	1.505139
C	-2.008926	6.910718	-0.832026
C	-2.798104	7.498624	1.76576
C	-2.974965	7.908411	-0.622768
H	-1.673468	6.646119	-1.836541
C	-3.38129	8.208995	0.699468
H	-3.093697	7.720691	2.794172
H	-3.397885	8.43763	-1.480804
H	-4.131956	8.980458	0.891989
N	0.188561	4.824761	-2.051675
C	-0.508973	4.050115	-2.946847
C	1.140111	5.716648	-2.540457
C	-0.299232	4.1293	-4.333277
H	-1.240105	3.362486	-2.518931
C	1.387774	5.828935	-3.927808
C	0.666651	5.032676	-4.837583
H	-0.880715	3.488719	-5.001636
H	2.140499	6.530643	-4.295804
H	0.852508	5.111375	-5.91224
N	1.314919	3.129462	0.006303
C	0.738664	1.859241	-0.001705
C	2.691234	3.209503	-0.000622
C	1.533355	0.702853	-0.010994
C	3.521558	2.09101	-0.006621
H	3.112794	4.217043	0.003402
C	2.963817	0.764076	-0.013209
H	1.0513	-0.279419	-0.017934
H	4.602946	2.24942	-0.011335
C	-3.739658	-0.455403	0.022658
H	-3.15881	-1.386763	0.039218
C	3.739792	-0.455338	-0.022642
H	3.15895	-1.386707	-0.039287
C	-5.126199	-0.531224	0.012333

H	-5.694267	0.410825	-0.005217
C	5.126327	-0.531163	-0.012341
H	5.694408	0.410884	0.00517
C	5.942847	-1.723691	-0.020518
C	7.370194	-1.593178	-0.016729
C	5.413966	-3.057078	-0.030808
C	8.217905	-2.702367	-0.02082
H	7.811848	-0.588798	-0.024201
C	6.247482	-4.174919	-0.046065
H	4.330432	-3.216827	-0.011091
C	7.67668	-4.029019	-0.040097
H	9.301913	-2.561843	-0.031449
H	5.813086	-5.178341	-0.037866
C	-5.942751	-1.72373	0.020507
C	-5.413903	-3.057132	0.030902
C	-7.370086	-1.593165	0.016609
C	-6.247455	-4.174943	0.046134
H	-4.330373	-3.21691	0.011311
C	-8.217836	-2.702328	0.02069
H	-7.811701	-0.58877	0.023996
C	-7.676651	-4.028992	0.040053
H	-5.8131	-5.178381	0.037997
H	-9.30184	-2.561769	0.031264
N	8.51565	-5.154848	-0.047444
N	-8.51565	-5.154783	0.047381
C	8.054403	-6.436431	-0.542547
C	7.399139	-6.525273	-1.79755
C	8.298963	-7.609438	0.21465
C	6.978868	-7.78239	-2.281138
H	7.239137	-5.620388	-2.393464
C	7.881494	-8.862659	-0.280798
H	8.811863	-7.535705	1.178928
C	7.217727	-8.955062	-1.526649

H	6.482816	-7.848394	-3.255312
H	8.072097	-9.766371	0.307369
H	6.89893	-9.930145	-1.90898
C	9.882698	-5.077493	0.430411
C	10.166786	-4.496975	1.692894
C	10.930979	-5.620406	-0.353705
C	11.497991	-4.448946	2.15797
H	9.350352	-4.10262	2.307222
C	12.258035	-5.574166	0.123211
H	10.704764	-6.072506	-1.324693
C	12.547983	-4.986478	1.376803
H	11.71318	-4.007583	3.136848
H	13.06571	-5.993025	-0.485981
H	13.578927	-4.954184	1.743721
C	-9.882738	-5.077399	-0.430389
C	-10.16689	-4.496883	-1.692852
C	-10.93097	-5.620286	0.353808
C	-11.498124	-4.448853	-2.157849
H	-9.350488	-4.102519	-2.30722
C	-12.258057	-5.574036	-0.123021
H	-10.704683	-6.072378	1.324782
C	-12.548068	-4.986368	-1.376609
H	-11.713372	-4.007504	-3.13672
H	-13.065702	-5.992867	0.486228
H	-13.579034	-4.954071	-1.743468
C	-8.054468	-6.436397	0.542488
C	-7.399422	-6.525303	1.797604
C	-8.298889	-7.609352	-0.214824
C	-6.979223	-7.782442	2.281197
H	-7.23954	-5.620438	2.393581
C	-7.881486	-8.862599	0.280626
H	-8.811638	-7.535571	-1.179179
C	-7.217938	-8.955066	1.526587

H	-6.48335	-7.848498	3.255456
H	-8.07197	-9.766285	-0.307621
H	-6.899199	-9.930176	1.908901

Table S7. Extinction coefficient of **7** in water.

Compound	λ_{max} in nm, (ε in $M^{-1}cm^{-1}\cdot10^3$)
4	290 (123.7), 317 (68.2), 439 (65.9), 494 (56.7), 630 (0.46)

Table S8. Cell permeability of the metal complex investigated in a parallel artificial membrane permeability assay. All data are presented as mean ± standard deviation.

Compound	Cell Permeability / μm/s
4	0.042±0.003
commercial highly permeable substance	0.055±0.005
commercial medium permeable substance	0.028±0.004
commercial poorly permeable substance	0.009±0.002